

<b>Name</b>	<b>Affiliation</b>
Ankur R. Desai*	Dept of Atmospheric and Oceanic Sciences, University of Wisconsin-Madison
Susanne Wiesner	Dept of Biological Systems Engineering, University of Wisconsin-Madison
Jonathan Thom	Space Science and Engineering Center, University of Wisconsin-Madison
Brian J. Butterworth	1=Cooperative Institute for Research in Environmental Sciences, CU Boulder, 2=
Nikaan Koupaei-Abyazani	Dept of Atmospheric and Oceanic Sciences, University of Wisconsin-Madison
Aronne Merrelli	Dept of Climate and Space Sciences and Engineering, University of Michigan
Bailey Murphy	Dept of Atmospheric and Oceanic Sciences, University of Wisconsin-Madison
Andi Muttaqin	Dept of Atmospheric and Oceanic Sciences, University of Wisconsin-Madison
Sreenath Paleri	Dept of Atmospheric and Oceanic Sciences, University of Wisconsin-Madison
Ammara Talib	Dept of Civil and Environmental Engineering, University of Wisconsin-Madison,
Jess Turner	Freshwater & Marine Sciences, University of Wisconsin-Madison
James Mineau	Dept of Atmospheric and Oceanic Sciences, University of Wisconsin-Madison
Paul Stoy	Dept of Biological Systems Engineering

\*Corresponding author: Ankur Desai, University of Wisconsin-Madison, Madison, WI 53706 USA, [desai@aos.wisc.edu](mailto:desai@aos.wisc.edu), +1-608-520-0305, <https://flux.aos.wisc.edu>

## Abstract

Long-running eddy covariance flux towers provide insights into how the terrestrial carbon cycle operates over multiple time scales. Here, we evaluated variation in net ecosystem exchange (NEE) of carbon dioxide ( $\text{CO}_2$ ) across the Chequamegon Ecosystem-Atmosphere Study (ChEAS) Ameriflux core site cluster in the upper Great Lakes region of the USA from 1997-2020. The tower network included two mature hardwood forests with differing management regimes (US-WCr and US-Syv), two fen wetlands with varying exposure and vegetation (US-Los and US-ALQ), and a very tall (400 m) landscape-level tower (US-PFa). Together, they provided over 70 site-years of observations. The 19-tower CHEESEHEAD19 campaign centered around US-PFa provided additional information on the spatial variation of NEE. Decadal variability was present in all long-term sites, but cross-site coherence in interannual NEE in the earlier part of the record became decoupled with time. NEE at the tall tower transitioned from carbon source to sink to a more variable period over 24 years. Respiration had a greater effect than photosynthesis on driving variations in NEE at all sites. A declining snowpack offset potential increases in assimilation from warmer springs, as less-insulated soils delayed start of spring green-up. No direct  $\text{CO}_2$  fertilization trend was noted in gross primary productivity, but influenced maximum net assimilation. Direct upscaling of stand-scale sites led to a larger net sink than the landscape tower. These results highlight the value of clustered, long-term carbon flux observations for understanding the diverse links between carbon and climate and the challenges of upscaling observations.

## Plain Language Summary

The terrestrial biosphere features the largest global sources and sinks of atmospheric carbon. Changes in growing season length, disturbance frequency, human management, increasing atmospheric CO<sub>2</sub> concentrations, amount and timing of precipitation, and warmer air temperatures, the carbon cycle is changing. Observations from the global eddy covariance flux tower network have been key for diagnosing these changes. However, data from most sites are limited in length. Here, we explore how multi-decadal carbon flux measurements from a cluster of flux towers in forests and wetlands in the upper Midwest USA respond to environmental change. Despite the proximity of the sites, year-to-year variation in carbon fluxes was rarely similar between sites. Surprisingly, warmer winters promoting earlier snowmelt led to later spring green-up because soil temperatures were colder. Higher CO<sub>2</sub> and warmer temperatures were not evident in the carbon fluxes but in parameters that influence carbon flux sensitivity to climate. Mismatch in flux measurements from a very tall tower flux to the network show that the whole does not seem to be simply a sum of its measured parts. More elaborate approaches may be needed to understand the processes that control carbon fluxes across large landscapes.

## Key Points

1. Multi-decade eddy covariance flux tower site cluster provides insight into variation of regional carbon cycling
2. Seasonal to decadal variation in two forests, two wetlands, and a tall tower responded differently to climate, phenology, and disturbance
3. Two dozen co-located towers over one summer did not upscale to tall tower landscape carbon flux, implicating several upscaling frontiers

## Keywords

Carbon fluxes, Ameriflux, CHEESEHEAD19, eddy covariance, forests, wetlands

## AGU Index Terms

0428 Carbon cycling, 0439 Ecosystems, structure and dynamics, 0438 Diel, seasonal, and annual cycles, 0497 Wetlands, 0426 Biosphere/atmosphere interactions

## 1. Introduction

The terrestrial ecosystem carbon cycle responds to and contributes to ongoing global changes (Friedlingstein *et al.*, 2020). Increasing CO<sub>2</sub> concentrations, longer growing seasons, changing frequency of extreme climate events, and shifts in disturbance regimes – among other factors – are leading to variations and

trends in net carbon uptake from ecosystem to global scales (Luo, 2007). For mid-latitude temperate and boreal ecosystems, documented leading drivers of carbon cycle change include shifts in photosynthetic efficiency, decomposition rate, temperature sensitivities, leaf phenology, water table depth, and plant mortality rates (Grimm *et al.*, 2013; Kasischke *et al.*, 2013; Keeling *et al.*, 1996; Luo *et al.*, 2004). Given the complexities of these drivers and their interactions, the terrestrial carbon cycle is a major source of uncertainty in future climate change projections (Friedlingstein *et al.*, 2006, Meehl *et al.*, 2007).

One of the critical observing systems that can directly monitor ecosystem carbon cycling are eddy covariance (EC) flux towers (Baldocchi, 2014). Since their advent and especially with the establishment of monitoring networks such as Ameriflux and FLUXNET, eddy covariance has held promise as a reliable benchmark for interannual to decadal changes to carbon cycling (Stoy *et al.*, 2009) and linking those changes to processes and mechanisms (Novick *et al.*, 2018). As a result, hundreds of formally registered sites and thousands of other sites now record carbon fluxes around the world (Burba, 2019). However, most direct observations of ecosystem carbon flux are rarely of sufficient length to disentangle and partition the driving factors by which the carbon cycle responds to environmental change (Hollinger *et al.*, 2021). Sites with more than ten years of public data are still relatively few, as sites have come online and gone offline with vagaries of funding availability, research questions, and data sharing policies, while new long-term focused projects with eddy covariance observations such as the U.S. National Ecological Observatory Network (NEON) or the European Union Integrated Carbon Observing System (ICOS) are relatively recent innovations (Loescher *et al.*, 2022).

Among long-running sites, an even smaller subset includes a set of co-located towers spanning gradients in land use and species composition, and virtually none have co-located replicate sites. The Chequamegon-Ecosystem Atmosphere Study (ChEAS) was established in the mid-1990s in a northern Wisconsin USA mixed forest and wetland landscape, representative of many temperate ecosystems (Davis *et al.*, 2003). ChEAS started with the establishment of eddy covariance observations on the WLEF-TV transmitter (US-PFa) in 1996 (Berger *et al.*, 2001), and subsequently expanded with towers in hardwood forests (US-WCr in 1998 and US-Syv in 2001) and wetlands (US-Los in 2000 and US-ALQ in 2014). Several shorter-term studies led to additional single-year deployments of towers at sites in the surrounding wetlands, forests, and lakes (Desai *et al.*, 2008a; Gorsky *et al.*, 2021). A short-term study recently included a large deployment of 19 towers in a 10 x 10 km domain surrounding US-PFa for four months in summer 2019. These were used to compare carbon fluxes in similar sites and upscale fluxes from individual ecosystems (Butterworth *et al.*, 2021).

As a result of this investment in multi-tower, long-term fluxes, we can investigate interannual to interdecadal variation in carbon assimilation and respiration across ecosystems experiencing the same climate, and how those relate to climate and biological forcings (Desai, 2010). Further, we can then link this to

shorter-term extensive tower networks to assess how representative the long-term towers are of the landscape and how spatial variability differs from the temporal variability of the carbon cycle.

Interannual variability in ecosystem-atmosphere carbon fluxes might result from changes in climate, ecosystem composition, and phenology (Fu *et al.*, 2019; Marcolla *et al.*, 2017; Piao *et al.*, 2020) and is poorly resolved in terrestrial ecosystem models (Keenan *et al.*, 2012). To determine the causes of this variability in CO<sub>2</sub> fluxes, it is necessary to study the terms that determine the net ecosystem exchange (NEE) of CO<sub>2</sub>: gross primary photosynthesis (GPP) and autotrophic and heterotrophic respiration, combined as ecosystem respiration ( $R_{eco}$ ) (Baldocchi *et al.*, 2018). Interannual variations in NEE arise from the influence of climate, land use, and physiology on GPP and  $R_{eco}$ . For example, drought can inhibit ecosystem productivity by reducing the strength of the terrestrial carbon sink and changing soil respiration rates (Piao *et al.*, 2019b). Similarly, climate change-driven water deficiency can promote forest tree species to alter leaf structures by increasing the percentage of defoliation (Carnicer *et al.*, 2011).

Moisture impacts can also extend beyond the soil to changes in atmospheric dryness arising from global warming (Grossiord *et al.*, 2020; Novick *et al.*, 2016). Diurnal temperature differences between day and nighttime temperatures can decrease due to increasing cloud cover, humidity, and rainfall at night (Cox *et al.*, 2020), and can lead to changes in the timing of leaf senescence (Wu *et al.*, 2018). Changes in nighttime temperatures also lead to alterations in the vapor pressure deficit (VPD) which was shown over longer timescales to be a strong modulator of tree growth in many ecosystems (Fu *et al.*, 2022; Restaino *et al.*, 2016).

Some of these ecosystem functions and their impact on interannual variation may also be captured by simple parameters, including maximum realized productivity, water-use efficiency, and carbon-use efficiency (Ballantyne *et al.*, 2021; Migliavacca *et al.*, 2021). Briegel *et al.* (2020) demonstrated that late winter and spring air temperature and summer precipitation indirectly influenced NEE. Seasonal and short-term conditions were found to be a better determinant of GPP and ecosystem respiration ( $R_{eco}$ ) interannual variability than annual climate variability. Of the two components, GPP has a stronger impact over the interannual variability of NEE than  $R_{eco}$  (Piao *et al.*, 2019b). Precipitation patterns and their resulting influence on longer-term soil moisture and elevated seasonal ecosystem metabolic rate (NEE, GPP,  $R_{eco}$ ) have been demonstrated in multiple studies (Jenerette *et al.*, 2008; Scott *et al.*, 2012; Vargas *et al.*, 2018). Other studies found that indirect effects of soil moisture explained 90% of the carbon uptake variability at the global scale, suggesting a strong soil water-atmosphere feedback, which was shown to be mainly driven by photosynthetic activity (Humphrey *et al.*, 2021). Furthermore, another study emphasized how temperature emerges as a leading factor for annual fluxes (Jung *et al.*, 2017).

Regionally, past studies found similar impacts on forest and wetland productivity over periods of time from five years to a decade (Desai, 2010; Desai *et al.*,

2010; Desai, 2014; Sulman *et al.*, 2009). Analysis of the carbon flux at US-PFa tall tower in Northern demonstrated the large GPP and equally large  $R_{eco}$  at the tall tower relative to stand-scale towers, contributing to a near-neutral NEE (Davis *et al.*, 2003). Leaf-out, leaf-fall, and soil freeze and thaw caused a strong seasonal pattern of NEE of  $CO_2$ . These results were further supported by Cook *et al.* (2004). GPP was not dependent on VPD unless it surpassed a high-level indicative of drier air.

Cluster sites also allow for tests of upscaling for regional fluxes. Aggregation of  $CO_2$  fluxes from a collection of sites in and around the Chequamegon-Nicolet National Forest in the summers of 2002 & 2003 demonstrated that footprint-weighted NEE,  $R_{eco}$ , and GPP at the tall tower were within 11% of the combined fluxes from 13 surrounding towers (Desai *et al.*, 2008a). Forest structure and age distribution strongly impact these fluxes, reflecting the history of land management and canopy complexity on modulating regional carbon cycle responses in forests (Desai *et al.*, 2005; Desai *et al.*, 2007; Murphy *et al.*, 2022). Wetlands and other aquatic landscapes (lakes, rivers, ponds) form more than a quarter of the landscape and have been shown to have unique responses to hydrologic change (Buffam *et al.*, 2011; Gorsky *et al.*, 2021; Pugh *et al.*, 2018; Turner *et al.*, 2021). These spatial scaling studies imply that the tower network should be sufficient for understanding stand and regional scale interannual variations in  $CO_2$  flux.

Here, we take advantage of the opportunity of having up to a quarter-century of quasi-continuous flux observations from a series of co-located plots and regional scale towers, to better understand drivers of the terrestrial carbon cycle. We ask: can we identify systematic trends or decadal variability in long-term regional NEE observations and their relationship to climatic trends? Are there systematic factors that link climate to site and landscape photosynthesis and ecosystem respiration, and are these trends coherent across sites? And finally, is site-level NEE representative of landscape-level flux in magnitude and inter-annual variability? By answering these questions, we can evaluate the temporal length and spatial extent of observations required to understand drivers of modes of variation in the terrestrial carbon cycle at scales relevant for Earth system modeling, landscape ecology, and global change.

## 2. Methods

### 2.1 Study region

We investigated long-term variation in terrestrial carbon exchange and their drivers across a mixed upland-lowland landscape located in the central part of North America in the U.S. state of Wisconsin (Figure 1). Northern Wisconsin is a heterogeneous and seasonally snow-covered landscape in the Dfb (warm-summer humid continental) Köppen climate zone. The mosaic of ecosystems ranges from old-growth, clear-cut, thinned forests, non-forested wetlands, lakes,

and open fields, including agriculture, with minimal urban/built-up land cover classes. The work here extends throughout much of northern Wisconsin, primarily within the confines of the Chequamegon-Nicolet, Ottawa National Forests, and surrounding public and private lands and Tribal Nations. The state's northern half is heavily forested and subject to active management (primarily northern hardwoods).

European settlement had an almost immediate, powerful impact on Wisconsin's vegetation (Rhemtulla *et al.*, 2009). Small scale Indigenous and subsistence logging of the dense pine forests quickly grew to large-scale logging as Indigenous inhabitants were forced to cede large chunks of resource-rich land throughout Wisconsin. The land was transformed by the booming timber industry, which led to the construction of levees, canals, and other hydrological manipulations. Not only was logging foundational to economic development in the region, but clear-cutting was preferential for the establishing farms, most of which were ultimately not successful (Gough, 1997). Railroad expansion and the market for pine-based paper further fueled the logging frenzy at the beginning of the 20<sup>th</sup> century. A handful of major events led to the end of intense logging in the region. Fire suppression was unsuccessful to control the tinderbox of logged forest floors littered with dry, dead heaps of tree branches and tops. A single fire in 1931 destroyed more than 30,000 ha of Wisconsin forest. To meet demand for local furniture, paper, and leather industries, the forests were being logged faster than they could recover. Drained soil nutrients and extreme droughts combined with other factors spelled an end to large-scale logging in Wisconsin. Less than one percent of Wisconsin's original old-growth forests remain today (Rhemtulla *et al.*, 2009).

Today, the landscape is dominated by mid to late successional even-aged northern hardwood forest stands consisting of aspen (*Populus* sp.) and birch (*Betula* sp.) in younger forests (~10% of the landscape), and maple (*Acer* sp.), ash (*Fraxinus* sp.), basswood (*Tilia americana*), eastern hemlock (*Tsuga canadensis*), and oak (*Quercus* sp.) in older forests (~20%). Drier sites can be dominated by evergreen, while conifer stands consist of red pine, balsam fir, or jack pine (~13%). Remnant old-growth stands of white pine (*Pinus strobus*) or eastern hemlock are present in smaller quantities. Among lowlands, an equal mix of shrub or grassy fens, fed by groundwater or streams, and nutrient-poor bogs cover nearly 30% of the landscape, generally blanketed in peat, with a canopy comprised of black spruce (*Picea mariana*, ~15% of wetland area), white cedar (*Thuja occidentalis*, ~12%), tamarack (*Larix* sp.) (~19%), or black ash (*Fraxinus nigra*). Sedges (e.g., *Carex* sp.), reeds and grasses, and sphagnum mosses are some examples of dominant understory vegetation in Wisconsin fens and bogs. Lakes and aquatic features cover 8.5% of the study region (Wisconsin Department of Natural Resources, 2016). Approximately 65% of the soils within the region are classified as deep, well-draining gravelly sands and moderately fine soils, with ~30% of soils categorized as having low and high infiltration rates when water levels are high and low, respectively. (Soil Survey Staff, 2022).

## 2.2 Flux tower sites

Long-term net ecosystem exchange and meteorological observations were made at five research sites that are part of the Department of Energy Ameriflux Network Management Program Chequamegon Ecosystem-Atmosphere Study (ChEAS) core site cluster (Table 1). These sites span a very tall regional flux tower (US-PFa), a managed and unmanaged forest (US-WCr and US-Syv), and two fen wetlands of contrasting spatial scale (US-Los and US-ALQ). Short site descriptions are provided below, with additional details in references cited within. Additionally, a short-term experiment of a larger number of towers was conducted in summer 2019, used here to place carbon cycle variability in context, and also described below.

Regional fluxes are observed from the Park Falls WLEF (US-PFa) tall tower. WLEF is a 447 m television tower surrounded by a mixed hardwood upland forest, wetlands and pine forests. The tower was instrumented by the National Oceanic and Atmospheric Administration (NOAA) for greenhouse gas observations in 1995 (Bakwin *et al.*, 1998) and since the middle of 1996, has been operating nearly continuously as an eddy covariance flux tower (Berger *et al.*, 2001). Here, US-PFa is used as an estimate of the regional CO<sub>2</sub> flux, given its mean footprint size of 5-10 km (Davis *et al.*, 2003). The tower has matching flux instruments at three height levels: 30 m, 120 m, and 390 m. The three systems were updated with new instrumentation in 2019. The current configurations include ATI Type-K sonic anemometers, LI-COR, Inc. LI-7200 infrared gas analyzers, and Vaisala, Inc. HMP155 temperature and relative humidity sensors. Data are collected with a Campbell Scientific CR6 data logger. Previous systems used LI-COR LI-6262 infrared gas analysers to measure CO<sub>2</sub> and H<sub>2</sub>O. Surface meteorological measurements include incoming solar, photosynthetically active radiation (PAR), 2 m air temperature and humidity, and precipitation. CO<sub>2</sub> concentration profile measurements were made by NOAA Earth System Research Laboratories using LI-COR LI-7000 infrared gas analyzers (Andrews *et al.*, 2014). CH<sub>4</sub> flux measurements were initiated in 2009 using a Picarro, Inc. 2301-f fast methane analyzer at 122 m (Desai *et al.*, 2015b).

The forest sites cover a representative managed mature hardwood forest (US-WCr), located typically outside the tall tower footprint, and an old-growth unmanaged forest representative of pre-settlement mesic stands (US-Syv) in Michigan’s western Upper Peninsula. Willow Creek (US-WCr) is a deciduous broadleaf forest dominated by basswood, sugar maple (*Acer saccharum* Marsh.), and green ash (*Fraxinus pennsylvanica* Marsh.), with an average stand age approaching 90 years (clear-cut in 1930s), established as a flux tower site in late 1999 (Cook *et al.*, 2004; Cook *et al.*, 2008). The lower canopy consists of sugar maple and ironwood (*Ostrya virginiana*) saplings, leatherwood maidenhair (*Dryopteris marginalis*), bracken ferns, and blue cohosh (*Caulophyllum thalictroides*). The elevation above sea level and flux footprint are approximately 515 m and 0.6 km, respectively. Average canopy height is 24 m and leaf area index is 5.3. The 30 m tower has flux measurements at 29.6 m using a Campbell Scientific (CSI)

CSAT-3 sonic anemometer and LI-COR, Inc. LI-7200 gas analyzer. The tower also includes profile measurements for PAR, temperature, humidity, winds, and CO<sub>2</sub>. Surface measurements include soil moisture, soil temperature profiles and heat flux. Soil temperature was measured at four depths within the soil profile at US-WCr; 2 cm, 5 cm, 10 cm, and 30 cm. In 2013, a commercial thinning harvest occurred in the area including the tower footprint, leading to removal of 30% of biomass over the course of two winters.

The Sylvania wilderness site (US-Syv) is an old-growth primary forest in the upper peninsula of Michigan, established with eddy covariance flux measurements in mid-2001 (Desai *et al.*, 2005). It consists of tree age ranges from 0 to 350 years old. Dominant overstory tree species are eastern hemlock (*Tsuga canadensis*) and sugar maple. Other trees in the tower footprint include basswood, yellow birch (*Betula alleghaniensis*), and ironwood. Average elevation is ~540 m. The tower measures fluxes at 37 m (recently lowered to 33.5 m due to tree mortality damage to the tower) using a CSAT-3 sonic anemometer and LI-7200 gas analyzer. Meteorological and soil profile measurements are similar to US-WCr.

The two wetland sites are both fen wetland sites representative of stream or groundwater fed wetlands across the region. Lost Creek (US-Los) is a stream-fed wetland with eddy covariance observations established in 2000 (Sulman *et al.*, 2009). Lost Creek is dominated by shrub species at an elevation of ~480 m. The site experiences significant peat accumulation due to the consistent source of water provided by the creek and associated floodplain. Vegetation comprises of alder, willow, and sedges. This wetland shares many of the characteristics of a typical minerotrophic wetland in the Great Lakes region. The 10 m flux tower measures CO<sub>2</sub>, H<sub>2</sub>O, and CH<sub>4</sub> fluxes using a Campbell Scientific, Inc. CSAT-3 sonic anemometer, and LI-COR, Inc. LI-7500 and LI-7700 gas analyzers. Meteorological measurements include air temperature, relative humidity, net radiation, PAR, and precipitation. Additional measurements include pCO<sub>2</sub>, soil temperature, and water level height.

US-ALQ is a peat and sedge fen near Allequash Creek (elevation ~ 500 m), part of the Flambeau River Basin in the Northern Highlands region and is also a North Temperate Lakes Long Term Ecological Research study site (Benson *et al.*, 2006; Turner *et al.*, 2019; Turner *et al.*, 2021). The wetland is predominantly peat and covers 32 hectares of the Trout Lake basin. The soil consists of highly conductive outwash sand on top of crystalline bedrock, promoting groundwater discharge to Allequash Creek. The creek flows downstream through the wetland and drains into Allequash Lake. The vegetation is dominated by tussock sedge (*Carex stricta*), leatherleaf shrub (*Chamaedaphne calyculata*), and sphagnum moss, with black spruce (*Picea mariana*), balsam fir (*Abies balsamea*), alder (*Alnus incana*), and tamarack (*Larix laricina*) adjacent to the hillslope bordering the wetland (Creswell *et al.*, 2008; Desai *et al.*, 2015b; Lowry, 2008), and narrow-leaved persistent emergent/wet meadow. Here, the tower is a 2 m tripod located within the wetland near the stream. CO<sub>2</sub>, CH<sub>4</sub>, and H<sub>2</sub>O fluxes



are measured with CSAT3, LI-7500, and LI-7700 instruments. Air temperature, relative humidity, and net radiation meteorological measurements are also made. Other ancillary measurements include  $p\text{CO}_2$ , and stream discharge at a nearby USGS stream gauge.

In June to October 2019, 19 additional flux towers were deployed in a quasi-random sampling of a 10 x 10 km box around the US-PFa tall tower as part of the Chequamegon Heterogenous Ecosystem Energy-balance Study Enabled by a High-density Array of Detectors 2019 (CHEESEHEAD19) experiment. Each temporary eddy covariance flux tower had similar instrumentation. These sites sample a broader range of forests, wetlands, and lakes in the landscape that contributed to the scaling goals of the CHEESEHEAD19 study (Butterworth *et al.*, 2021), and included recent clear-cuts to older established forests. Site descriptions are provided at <http://cheesehead19.org> with further details in Butterworth *et al.*, (2021), Murphy *et al.* (2022), and Desai *et al.* (2021).

Additional daily and monthly meteorological data on regional precipitation and snowfall was acquired from the Minocqua, WI cooperative weather station and historical climate observing site (USC00475516) as accessed from the Midwest Regional Climate Center (<https://mrcc.purdue.edu/>).

### 2.3 Physiological parameter estimation

We estimated parameters of photosynthetic activity and respiration using Equation 1, which links the relationship of maximum photosynthetic activity ( $A_{\text{max}}$ ), quantum yield ( $\Phi$ ), dark respiration ( $R_d$ ), and photosynthetic active radiation (PAR), as well as via Equation 2 regarding the relationship of  $Q_{10}$ , air temperature ( $T_{\text{air}}$ ), and base respiration at 10 °C ( $R_{10}$ ) to respiration as follows:

$$NEE = \frac{\alpha \times PAR \times A_{\text{max}}}{\alpha \times PAR + A_{\text{max}}} - R_d \quad (1)$$

and

$$Reco = R_{10} \times Q_{10}^{\left(\frac{T_{\text{air}} - 10}{10}\right)} \quad (2).$$

All parameters were estimated using nonlinear models via the nls function in R (R Core Team, 2021) which fits nonlinear least-square estimates.

### 2.4 Phenology observations

The timing of phenological events such as leaf-on and leaf-off as well as the span of time between these events captures the influence of a suite of climatological drivers and plays a significant role in determining carbon cycle dynamics. These include the uptake of atmospheric carbon through primary productivity and the movement of carbon between storage pools through leaf senescence and decomposition (Piao *et al.*, 2007) while also influencing processes related to plant water use (Fisher *et al.*, 2017; Mathias & Thomas, 2021; Raupach *et al.*, 2005). To relate interannual carbon flux observations to phenology, we integrated indicators of leaf emergence, maximum cover, and senescence as derived from

cameras mounted on three sites as part of the Phenocam project (Richardson *et al.*, 2018).

Phenology data were collected at US-WCr, US-Los, and US-Syv using high-frequency half-hourly visible wavelength digital time-lapse imagery from a camera (referred to as a ‘PhenoCam’) mounted on the EC flux towers. Cameras are set to a fixed white balance above the level of the vegetation canopy for a landscape-level field of view. The cameras are positioned at a slight decline (between 20°–40°) and are north-oriented to minimize lens flare, shadows, and forward scattering of light from the vegetation canopy. Observations are sent to a central server every half hour for processing and archival (Seyednasrollah *et al.*, 2019). These images are then masked by region of interest (ROI) for dominant land cover vegetation components. From the masked images, a green chromatic coordinate ( $G_{CC}$ ) is calculated.  $G_{CC}$  is a dimensionless index that corresponds to the ratio of green in an image composed of red, green, and blue color channels (Keenan *et al.*, 2014). For US-Syv, two regions of interests (ROI) were applied to separate evergreen from deciduous cover. Here, we focus on the deciduous ROI.

## 2.5 Data Analyses

Flux data were processed according to standard conventions (Table 1). Raw data corrections and quality control were based mostly on algorithms for calibration, sonic rotation, lagged covariance, spectral correction, and data filtering as detailed in Berger *et al.* (2001), with additional processing through EddyPro (LI-COR, Inc.) software. Hourly (US-PFa) or half-hourly (US-WCr, US-Los, US-Syv, US-ALQ, CHEESEHEAD) averaged flux and meteorological observations output from these algorithms were then quality controlled for spikes, shifts, spurious trends from sensor degradation and calibration changes, and reviewed and passed through the Ameriflux data quality assurance and quality control process (Pastorello *et al.*, 2020). Net ecosystem exchange (NEE) observations of  $CO_2$  flux were storage-corrected with  $CO_2$  concentration profiles.

Gap-filling of missing observations and those removed by friction velocity thresholds were consistently filled at all sites using marginal distribution sampling (MDS) as implemented in REddyProc (Wutzler *et al.*, 2018). The nighttime partitioning method (Reichstein *et al.*, 2005) was used to partition NEE into components Gross Primary Productivity (GPP) and Ecosystem Respiration ( $R_{eco}$ ). Consistent gap-filling, variable selection, and partitioning ensure robust cross-site comparisons (Desai *et al.*, 2008b).

Monthly, seasonal, and annual totals of NEE, GPP, and  $R_{eco}$  were then calculated for each site, along with average air temperature, vapor pressure deficit, shortwave incoming radiation, precipitation (including snowfall), and soil temperature. Only full-year data were used for each site. Uncertainties for NEE were calculated using the variable  $u^*$  approach used for the FLUXNET2015 database, which involves calculating systematic and random uncertainty and

then reporting the 25th and 75th percentile threshold of NEE as the uncertainty range (NEE\_VUT\_25 and NEE\_VUT\_75). Uncertainty of GPP and  $R_{eco}$  were assumed to be 20% of the mean flux equally distributed around mean, a range based on comparison of gap-filling and partitioning method uncertainty reported in Desai *et al.* (2008a).

Growing season length and seasonal start and end dates were estimated from the PhenoCam imagery. Growing season start and end dates were estimated based on the  $G_{CC}$  running three-day average. Using a threshold crossing approach, we identified start and end of season for 10% of the rising or falling maximum amplitude of average  $G_{CC}$  values, respectively (Richardson *et al.*, 2018).

To estimate the effects of climate drivers on fluxes, we conducted seasonal and annual regression analyses on the fluxes and on the parameters of the flux partitioning, including values of maximum light-limited assimilation ( $A_{max}$ ) for photosynthesis and respiration temperature sensitivity ( $Q_{10}$ ) for each site-month. First, we estimated annual models of NEE, GPP,  $R_{eco}$ , as well as  $A_{max}$ ,  $R_d$ ,  $Q_{10}$ , and  $R_{10}$ , to understand if seasonal variations (growing season, GS, defined as June-September, and non-growing season, NGS determined via phenological observations described in 2.4) in environmental variables affected the interannual variability of carbon fluxes. For annual models we also tested whether growing season length affected carbon fluxes and physiological variables, however this analysis was only possible for the sites US-WCr, US-Los, and US-Syv, as these were the only sites equipped with PhenoCams.

We used annual and seasonal averages of air temperature from the flux measurement levels ( $T_{air}$ ) above canopy at each tower and also a regional temperature estimate from the 396 m level of the tall tower ( $T_A$ ). For each site, in addition to temperature we also extracted VPD, precipitation, and snowfall, as well as annual values of  $CO_2$  measured at the top level of the tall tower, as drivers of annual averages of NEE, GPP, and  $R_{eco}$ . We included a factor of Site and Year; however, with environmental variables in the model, Year was not significant and is subsequently excluded. Next, we estimated monthly models of NEE, GPP, and  $R_{eco}$  to quantify how plant physiological drivers (i.e.,  $A_{max}$ ,  $Q_{10}$ ), affected intra-annual variability in carbon fluxes. Finally, we estimated monthly models of  $A_{max}$ ,  $Q_{10}$ , and  $R_d$  – which were primarily drivers of NEE – to understand their interactions with environmental drivers such as  $T_{air}$ , VPD, incoming shortwave radiation ( $R_g$ ), precipitation, and snow. We also included a factor for site and season to quantify differences in response magnitude by location and growing and non-growing season. Furthermore, we included a random factor and autocorrelation structure for month to account for autocorrelated dependent and independent variables.

For this analysis we analyzed data via segmented regression, as linear mixed models were not able to properly fit the non-linear response to temperature. Accordingly, we determined a breakpoint with  $T_{air}$  for each of the models via the “segmented” function from the “segmented” package in R (Muggeo, 2008). Significant drivers were determined based on p-values ( $<0.05$ ) and fit ( $r^2$  and

AIC). Accordingly, non-significant drivers were excluded on a consecutive basis. All linear and mixed models were analyzed via R using the nlme (Pinheiro *et al.*, 2022) and emmean packages (Lenth, 2022).

### 3. Results

#### 3.1 Multi-decade observations of regional climate

All study sites were in a single climatic region, though some variance occurs from differences in elevation and proximity to Lake Superior influencing primarily total snowfall. As noted from the US-PFa tower and nearby weather station observations, mean temperature reflected humid continental climate (Köppen classification Dfb) with mean annual temperature ( $T_A$ ) of 5.24 °C and annual precipitation of 852 mm including a mean annual snowfall of 226 cm (Table 2). However, interannual variation in those climatic values are large, with more than 4.5 °C range (maximum minus minimum) in mean annual temperature, 66% range in mean annual precipitation, and 124% range in snowfall over the 24-year record.

Overall, these variations were distributed evenly through the record and multi-year or decadal cycles were not evident (Figure 2). After 2006, a shift is observed toward generally wetter and cloudier conditions, but with less snowfall and warmer summers. Over the entire time period, CO<sub>2</sub> concentration increased by 13.7% (from 367.2 ppm to 418.7 ppm) in line with global trends.

Beyond the strong trend in CO<sub>2</sub> concentration increase of 2.11 ppm yr<sup>-1</sup> [Theil-Sen slope 95% confidence 2.06-2.16, Kendall  $\tau$  =1,  $p$ <0.01], other trends, including significant trends in climate, were less evident (Table 3). At the tall tower (US-PFa), summer air temperature ( $T_A$ ) significantly increased 0.056 °C yr<sup>-1</sup> [95% confidence 0.028,0.077,  $\tau$  =0.30,  $p$ =0.037]. Mean decadal average summer  $T_A$  at the start of the record (1997-2006) of 16.14 +/- 0.61 °C increased to 16.9 +/- 0.77°C during the final 10 years (2011-2020). This increase was coincident with a significant increase ( $p$ =0.03) in summer VPD from 4.88 +/- 0.90 kPa +/- to 5.88 +/- 0.78 kPa over the same time periods.

Co-op observing station precipitation and snow also had significant trends. Total annual precipitation increased 13.1 mm yr<sup>-1</sup> [8.1,17.4,  $\tau$  =0.33,  $p$ =0.02], leading to 23% greater precipitation in the last 10 years [964 +/- 165 mm] compared to the first 10 years [783 +/- 109 mm]. Meanwhile, total snowfall declined -7.2 cm yr<sup>-1</sup> [-9.8,-3.94,  $\tau$  =-.30  $p$ =0.04], leading to 43% decline in mean total snowfall from first 10 years [314 +/- 46 cm] to the last 10 years [179 +/- 71 cm]. While decreasing snowfall is distributed through fall, spring, and winter seasons, increasing precipitation is only significant in the autumn.

When pooled across all sites, a few trends were more evident (Table 3). In addition to the summer  $T_A$  trend at the tall tower, average seasonal  $T_{air}$  across the all sites showed the largest increase in the fall. Spring soil temperatures

decreased across all four measurement depths, with an average temperature change of  $-1.30\text{ }^{\circ}\text{C}$  between 1998 and 2020. The most pronounced change in spring soil temperature was at 2 cm depth, where temperatures decreased on average by  $0.08\text{ }^{\circ}\text{C year}^{-1}$  for a total cooling of  $1.93\text{ }^{\circ}\text{C}$  across the measurement period. The rate of temperature change at 5 cm, 10 cm, and 30 cm depths during spring were all around  $-0.04^{\circ}\text{C year}^{-1}$ .

### 3.2 Changing leaf phenology

While growing season length and timing changes were not available for the entire record, the PhenoCam observations at the two forest sites (US-WCr and US-Syv) and one wetland (US-Los) revealed a few interesting trends that potentially explain variations in carbon fluxes (Fig. 3). The two forest sites both reflect a regular seasonal cycle of spring green up in late May and leaf senescence by early October, though the start of season is typically a week later in the old-growth forest (US-Syv). At both sites, peak  $G_{CC}$  occurs early in the season, typically in early June, and declines over a four-month period. Generally, a pattern of declining NEE (increasing GPP) occurs shortly afterwards.

For both sites, high interannual variability of  $G_{CC}$  was observed around October at time of senescence, indicating a strong role of senescence as a driver of interannual variability of carbon fluxes. The wetland site (US-Los) was similar in most respects, except for an earlier start to green up in early May given the prevalence of sedge and shrub vegetation, though a similar timing for peak greenness as for the forest sites. Consequently, US-Los had the longest growing season at 153 days on average, followed by the US-Syv cohort (142 days), and US-WCr (140 days).

Growing season length decreased at all three sites (US-WCr, US-Los, US-Syv), with an average shortening of 4.1 days since the earliest phenocam record in 2012 (Table 3), with a significant decrease of 6 days from at US-Los ( $p < 0.05$ ) and a weaker decrease of 4.6 days from 2016 to 2020 at US-Syv, though the trend was not statistically significant ( $p = 0.0626$ ). Similarly, while the the observed decrease in growing season length at US-WCr from 2012 to 2020 was not significant ( $p = 0.99$ ), there is an observed change from 2016 to 2020 of a decrease of 4.3 days ( $p = 0.0651$ ). Interannual variability in growing season length was similar across all three sites, with an average standard deviation of 10.5 days.

The shortening of the growing season observed at sites US-WCr and US-Los was driven primarily by a later start to spring leaf out, with a significant average yearly shift of 2.63 days. However, leaf off dates also occurred earlier in the growing season, with a significant average yearly shift of 0.79 days. At US-Syv, changes in growing season length were fairly equally driven by a later start to leaf out and an earlier start to leaf off with an significant average yearly shift of 2.5 and 2 days, respectively. The greatest interannual variability in leaf out dates was observed at US-Los ( $SD = 5.75$  days), while US-Syv experienced the

least variability among years ( $SD = 3.31$  days).

US-WCr also experienced the greatest interannual variability in leaf off dates ( $SD = 4.84$  days), while US-Los experienced the least ( $SD = 3.30$  days). Leaf out at US-WCr began 12 days later in 2020 than it did in 2012 when the data record began, with an average yearly change in leaf out date of 1.5 days later in the season. The transition to senescence began 3 days earlier in 2020 than it did in 2012, with an average yearly change of 0.38 days. US-Los leaf out began 15 days later in 2020 than it did in 2016 when the data record began (no leaf out data was available for 2015), with an average yearly change in leaf out date of 3.75 days later in the season. The transition to senescence began 6 days earlier in 2020 than it did in 2015, with an average yearly change of 1.2 days. Leaf out began at US-Syv 10 days later in 2020 than it did in 2016 when the data record began (no leaf out data was available for 2015), with an average yearly change in leaf out date of 2.5 days later in the season. The transition to senescence began 10 days earlier in 2020 than it did in 2015, with an average yearly change of 2 days.

Shifts in timing of spring also led to shifts in timing of maximum  $G_{CC}$ . The timing of maximum annual  $G_{CC}$  generally occurred between late May and mid July depending on the dominant vegetation type, but at all three sites the date of maximum  $G_{CC}$  shifted later in the season over the observation record, with an average yearly shift of 4.64 days. This shift aligns with the later start to leaf-out observed at all three sites. Temperature was also significantly correlated with  $G_{CC}$  across the sites, with increases and decreases in temperature corresponding to increases and decreases in  $G_{CC}$ , respectively.

### 3.3 Response of the carbon cycle

The five long-term flux towers showed a large range of mean annual NEE (Table 4). The tall tower (US-PFa) regional NEE estimate averaged to near zero ( $-3.74$   $gC\ m^{-2}\ yr^{-1}$ ) over the 24-year period. In contrast, all of the stand scale towers exhibited far more years as carbon sinks, and generally had a modest to large mean net annual uptake of carbon, with the largest in the mature hardwood forest (US-WCr,  $-253$   $gC\ m^{-2}\ yr^{-1}$ ), followed by the old-growth forest (US-Syv,  $-118$   $gC\ m^{-2}\ yr^{-1}$ ), and smallest in the two wetland sites (US-Los,  $-91.1$   $gC\ m^{-2}\ yr^{-1}$  and US-ALQ,  $-84.6$   $gC\ m^{-2}\ yr^{-1}$ ). Gaps in these records reflect years without continuous data due to sensor malfunction or lapses in funding. The discrepancy in site to regional NEE is most evident in mean annual GPP, which is lower at the regional scale ( $877$   $gC\ m^{-2}\ yr^{-1}$ ) than any of the stand-scale sites. The old-growth forest showed largest mean GPP ( $1340$   $gC\ m^{-2}\ yr^{-1}$ ) followed by the managed mature forest ( $1174$   $gC\ m^{-2}\ yr^{-1}$ ), while the wetlands were smaller (US-Los,  $963$   $gC\ m^{-2}\ yr^{-1}$  and US-ALQ,  $997$   $gC\ m^{-2}\ yr^{-1}$ ).  $R_{eco}$  for the region ( $878$   $gC\ m^{-2}\ yr^{-1}$ ) was similar to the wetlands ( $962$  to  $997$   $gC\ m^{-2}\ yr^{-1}$ ) and mature forest ( $918$   $gC\ m^{-2}\ yr^{-1}$ ), all of which were lower than the old-growth forest ( $1278$   $gC\ m^{-2}\ yr^{-1}$ ).

Interannual variation was present for all fluxes across all sites, though in varying degrees of magnitude and patterns (Fig. 4). At the regional scale (US-PFa), annual NEE was near-zero to a modest source through 2005 ( $68.8 \pm 59.4 \text{ gC m}^{-2} \text{ yr}^{-1}$ ). The following years from 2006 through 2012 featured primarily modest sinks ( $-98.9 \pm 52.5 \text{ gC m}^{-2} \text{ yr}^{-1}$ ) of similar magnitude to the prior source. The last eight years feature 2-3 year periods where net fluxes oscillated between source and sink, leading to a near neutral by high variance magnitude of annual NEE ( $-3.29 \pm 95.0 \text{ gC m}^{-2} \text{ yr}^{-1}$ ). The increasing sink from 2006 appears to have occurred despite a decrease in GPP over the same period, reflecting an even greater drop in  $R_{\text{eco}}$ , to as little as half the annual value observed in earlier years. GPP and  $R_{\text{eco}}$  both reached a nadir in 2009, and both slowly increased with high interannual positive correlation throughout ( $r=0.93$ ), a correlation much weaker ( $r = 0.38$  to  $0.67$ ) at the other sites excluding US-ALQ. The wetland site with decadal observations (US-Los) experienced less carbon interannual variability (SD:  $4.47 \text{ g C m}^{-2} \text{ day}^{-1}$ ) relative to the forest sites (US-Syv and US-WCr; SD:  $5.75 \text{ g C m}^{-2} \text{ day}^{-1}$  and SD:  $6.55 \text{ g C m}^{-2} \text{ day}^{-1}$ ). With respect to phenology, we observed an overall decreasing trend of NEE as  $G_{\text{CC}}$  increased during the growing season for all sites with PhenoCam observations.

US-WCr, as a closed-canopy mature hardwood forest, had the largest carbon sink that increased in magnitude with time outside of a few unique years. The unique years reflect events specific to US-WCr (Table 5). The late spring of 2001 included complete defoliation and reflushing of the canopy in June as a result of a forest tent caterpillar outbreak, followed by a warm summer. As a result of high  $R_{\text{eco}}$  from that event, the site was a carbon source. The site also had a reduced sink to small source from 2014-2015. During this period, a commercial thinning harvest occurred in the tower footprint, leading to removal of approximately 15% of the overstory biomass in the winter of 2012-2013 and a similar amount in winter of 2013-2014, as reflected in the large drop in GPP, followed by canopy release with an increase in GPP. Changes in  $R_{\text{eco}}$  are muted in comparison. The years following the harvest and recovery, after 2017, led to some of the largest carbon sink years in the record.

While mature forests have the largest carbon sinks, the old-growth forest had the larger GPP and  $R_{\text{eco}}$ , consistent with overall higher per area density of biomass and soil organic matter at the site. The seasonal cycle of NEE shows that while US-WCr has higher carbon emissions (positive NEE) in the shoulder seasons, US-Syv shoulder season NEE is partly offset by earlier photosynthetic activity in conifer species, followed by overall significantly higher respiration through the summer (Fig. 5). Growing season GPP is similar at both sites. Annual NEE at US-Syv was variable but maintained a carbon sink in most years. The increased carbon source in 2004-2005 was primarily a consequence of increasing non-growing-season  $R_{\text{eco}}$ . After the tower resumed data collection in 2011, NEE magnitudes were similar, but GPP and  $R_{\text{eco}}$  magnitudes were both larger. The site became a stronger sink for carbon after 2013, as  $R_{\text{eco}}$  declined faster than GPP, but switched back to a source in 2020. In 2019, the tower was struck by a large overstory tree in the tower footprint, leading to significant data outage

for half of the year. The resulting drop in GPP and increase in  $R_{eco}$  likely reflected the impact of that mortality event. Other mortality events include overstory tree mortality in late spring 2017 and the fall of a standing dead tree in November 2018 (Table 5).

The two wetland sites (US-Los and US-ALQ) both were steady carbon sinks throughout the record, though typically smaller in magnitude than the forests. In the three overlapping years, both sites had remarkably similar NEE magnitudes, and for two of those years, virtually the same GPP and  $R_{eco}$ , though seasonality varied (Fig. 5), with US-ALQ maintaining a small level of GPP throughout earlier and later in the growing season, reflective of greater sedge species activity. Total GPP and  $R_{eco}$  at both sites were lower than the forests. A slight increasing trend in  $R_{eco}$  and GPP is noted in US-Los from 2002-2008, during a period of significant water table decline. After the tower was restarted in 2014, magnitudes of GPP and  $R_{eco}$  were similar to the earlier period of the record, consistent with an increase in the water table comparable to previous years.

All sites had relatively similar diel cycles through the growing season (Fig. 6). Generally, GPP tracked solar radiation and peaked at noon, though it was slightly earlier and more asymmetric (greater GPP in daytime) at the tall tower.  $R_{eco}$  at all sites tracked temperature, which would be expected given the partitioning approach applied, and peaked 2-4 hours later. While at the forest and wetland sites, the offset in peak GPP and  $R_{eco}$  had limited effect on the diel cycle of NEE, which tracked GPP, at the US-PFa, the offset leads to an asymmetry in the diel cycle of NEE, leading to greater overall carbon uptake in the morning compared to the afternoon.

The CHEESEHEAD19 study affords an opportunity to evaluate how representative the long-term towers were with respect to quasi-randomly placed towers in forests, wetlands, lakes, and fields within the 10 x 10 km domain surrounding US-PFa (Fig. 7). Over the June-Sept 2019 period when all towers were operating, spatial variability in carbon uptake across similar vegetation types is evident. The long-term US-WCr site had uptake in June-Sept 2019 that was larger (more negative) than any of the CHEESEHEAD19 deciduous forests and only eclipsed by one evergreen site. However, interannual variations at US-WCr across all other observed June-Sept spans the entire range of spatial variability in forest CHEESEHEAD19 NEE. Meanwhile US-Syv 2019 NEE was near the median of CHEESEHEAD19 sites, with more muted interannual variation relative to spatial variation. Both US-WCr and US-Syv had lower GPP and lower  $R_{eco}$  than all CHEESEHEAD19 forests. Both long-term wetland sites, US-Los and US-ALQ had larger (more negative) NEE than the CHEESEHEAD19 wetlands in June-Sept, and similar to US-WCr, the long term June-Sept interannual variability at US-Los spans the range of CHEESEHEAD19 observed wetland NEE. Unlike the forests, US-Los and US-ALQ GPP and  $R_{eco}$  were of similar magnitude. Lakes in CHEESEHEAD19 had NEE closer to neutral or a source compared to the wetlands.



### 3.4 Drivers of carbon cycle variability

#### 3.4.1 Interannual

Several seasonal environmental factors were found by our model to explain interannual variation in NEE across the sites. An increase in winter rainfall and air temperature ( $T_{\text{air}}$ ) significantly increased NEE to more positive (reduced ecosystem carbon uptake and enhanced emission), whereas greater summer air temperatures significantly decreased NEE to more negative (enhanced ecosystem carbon uptake and reduced emission). For annual average GPP, we found a significant increase in GPP with greater summer VPD, while all other environmental variables in the model were not significant ( $p > 0.05$ ). Annual  $R_{\text{eco}}$  significantly increased with greater annual  $T_{\text{air}}$  and an increase in average winter VPD. However, greater summer  $T_{\text{air}}$  significantly decreased  $R_{\text{eco}}$ . Season length did not significantly affect NEE, GPP, or  $R_{\text{eco}}$ . No significant linear trends or relationship to atmospheric  $\text{CO}_2$  were found for NEE, GPP, or  $R_{\text{eco}}$  at any site (Table 3).

Several environmental factors indirectly influenced carbon fluxes through photosynthesis parameters. Annual maximum photosynthetic rate ( $A_{\text{max}}$ ) significantly increased with greater summer  $T_{\text{air}}$  (Figure 8). Furthermore,  $A_{\text{max}}$  was significantly greater at US-Syv compared to US-Los and US-PFa (by 1.3-1.5  $\mu\text{mol m}^{-2} \text{s}^{-1}$ ). In contrast, quantum yield ( ) was only significantly greater at US-WCr than other sites (Table 3).

Across respiration parameters, we found temperature sensitivity ( $Q_{10}$ ) significantly increased with greater winter precipitation and annual average VPD.  $Q_{10}$  was significantly greater at US-Syv than other sites. The base respiration ( $R_{10}$ ) significantly increased with winter precipitation, while greater winter temperatures decreased  $R_{10}$ .  $R_{10}$  was significantly greater at US-Los and US-PFa compared to US-ALQ and US-WCr, while US-PFa also had significantly greater  $R_{10}$  compared to US-Syv. Dark respiration ( $R_d$ ) significantly increased with greater winter snowfall and summer air temperature.  $R_d$  was significantly greater at US-Syv ( $2.2 \mu\text{mol m}^{-2} \text{s}^{-1}$ ) and US-PFa ( $1.7 \mu\text{mol m}^{-2} \text{s}^{-1}$ ) compared to US-WCr ( $0.8 \mu\text{mol m}^{-2} \text{s}^{-1}$ ) and US-Los ( $0.8 \mu\text{mol m}^{-2} \text{s}^{-1}$ ).

When we included season length in the models, higher  $\text{CO}_2$  and season length significantly increased magnitude of  $A_{\text{max}}$  (to more negative), while  $T_{\text{air}}$  was no longer significant. Seasonal length did not affect  $\alpha$ . For  $Q_{10}$ , season length and  $\text{CO}_2$  were not significant, though season length significantly increased  $R_{10}$ , with  $T_{\text{air}}$  and precipitation not significant anymore. Season length and  $\text{CO}_2$  significantly increased  $R_d$ .

#### 3.4.2 Intra-annual

Variability of parameters and carbon fluxes by season can also help explain site-level differences (Figure 9). During the growing season (GS), US-WCr had significantly greater carbon uptake compared to US-PFa, US-Syv, US-Los, and

US-ALQ. However, this ordering changes for the non-growing season (NGS), where US-PFa and US-ALQ had significantly more positive NEE compared to US-Syv and US-WCr, which were more similar.

These differences are also expressed in response parameters of  $A_{\max}$  and  $R_d$  (Figure 9b-c). As  $A_{\max}$  increases in magnitude, NEE among the sites diverged, forming three clusters, of US-PFa and US-ALQ with the smallest NEE, US-Los and US-Syv in the middle, and US-WCr with the largest. Relationships between  $R_d$  and NEE among sites are more similar in slopes, but steeper slopes lead to divergence in NEE across all sites when  $R_d$  exceeded  $6 \mu\text{mol m}^{-2} \text{s}^{-1}$ , with the exception of US-PFa which had significantly lower respiration than the other sites.

Comparisons of NEE sensitivity by season also reveal some differences (Figure 9d-f). Growing season NEE was less sensitive (smaller slope) to  $A_{\max}$  and  $R_d$  than non-growing season NEE, which includes shoulder seasons. In contrast, growing season NEE responded more strongly to  $Q_{10}$ . While  $A_{\max}$  was significantly greater at all sites compared to the non-growing season, there was no significant difference among sites (Figure 10). However, VPD and  $R_g$  moderated the magnitude of  $A_{\max}$  by site. US-Syv showed a significant increase in  $A_{\max}$  with greater VPD, and US-WCr a significant decrease.  $A_{\max}$  significantly increased only at US-WCr with greater incoming radiation ( $R_g$ ), resulting in significantly greater  $A_{\max}$  compared to all other sites except US-ALQ when  $R_g$  was  $> 400 \text{ W m}^{-2}$ . All other sites showed no significant changes in  $A_{\max}$  with VPD or  $R_g$ .  $A_{\max}$  also was related to monthly precipitation (negatively) and snowfall (positively). We also identified a breakpoint in  $T_{\text{air}}$  of  $7.4^\circ\text{C}$ , where at cooler temperatures, VPD and  $R_g$  had far weaker control on  $A_{\max}$  than with warmer temperature.  $\alpha$  was not significant in the model of NEE. We only found a significant increase in NEE with  $\alpha$  with temperature when  $T_{\text{air}}$  was  $> 3.2^\circ\text{C}$ , independent of site.

An increase in  $Q_{10}$  significantly reduced carbon uptake during the GS (by  $\sim 0.01 \mu\text{mol m}^{-2} \text{s}^{-1}$ ), while  $Q_{10}$  had a negligible effect on NEE during the NGS. The model of  $Q_{10}$  indicated that  $T_{\text{air}}$  significantly increased  $Q_{10}$  at US-Los, US-PFa, and US-Syv (Figure 11). At moderate temperatures ( $10^\circ\text{C}$ ) US-Los had lower  $Q_{10}$  compared to the other sites, while at warm temperatures ( $30^\circ\text{C}$ ) US-PFa had greater  $Q_{10}$  compared to US-Los and US-WCr. For colder temperatures ( $< -2.2^\circ\text{C}$ )  $Q_{10}$  decreased at all sites.  $Q_{10}$  also responded to VPD at US-PFa and site-level differences in  $Q_{10}$  with  $T_{\text{air}}$  and VPD are apparent. Precipitation significantly increased  $Q_{10}$  by 0.03-0.07, for all temperatures.

Like  $Q_{10}$ ,  $R_d$  expressed site-level responses as a function of temperature, VPD, and precipitation (Figure 12).  $R_d$  significantly increased NEE to more positive in the NGS (by  $\sim 1 \mu\text{mol m}^{-2} \text{s}^{-1}$ ) compared to the GS (by  $\sim 0.5 \mu\text{mol m}^{-2} \text{s}^{-1}$ ). Precipitation significantly increased dark respiration by  $\sim 0.03 \mu\text{mol m}^{-2} \text{s}^{-1}$ . Temperature significantly increased  $R_d$  at all sites except US-WCr, resulting in lower  $R_d$  compared to US-PFa, US-Syv, and US-Los when  $T_{\text{air}}$  was above  $1.5^\circ\text{C}$ .

However, when  $T_{\text{air}}$  was  $< 1.5^{\circ}\text{C}$  and VPD greater than 1.5 hPa, US-WCr had significantly greater  $R_d$  compared to US-PFa, US-Syv, and US-Los when  $T_{\text{air}}$  was  $< 1.5^{\circ}\text{C}$  and VPD was above 1.5 hPa. Greater VPD significantly decreased  $R_d$  at US-PFa and US-Syv.

## 4. Discussion

### 4.1 Annual to decadal variability in northern forests and wetlands

Our globally unique cluster of long-term towers measuring ecosystem carbon exchange afforded us an opportunity to evaluate interannual to interdecadal variations in net carbon exchange and evaluate drivers of those at all time scales. Decadal variability is present at all sites and suggests that extrapolations of trends, interannual variability magnitudes, and sensitivity to towers with shorter records should be interpreted with caution. While a large fraction of flux towers lack the necessary tenure to study decadal fluxes (Novick *et al.*, 2018), a growing number will reach those milestones soon (Baldocchi, 2020), further supported by the rise of sustained operations and long-term observing infrastructure (e.g., NEON). It is likely that our understanding of processes like  $\text{CO}_2$  fertilization, disturbance impacts on carbon uptake, and ecosystem temperature sensitivity will be significantly revised, with ramifications for Earth system model evaluation and parameterization.

Across our tower network in mixed upland-lowland temperate to boreal transition managed ecosystems, we find a variety of responses. At the regional scale, we observed substantial interdecadal variability at the very tall tower, one of the longest continuous flux tower records on the globe. Over the initial 16 years (1997-2013), the measured landscape carbon uptake switches from a small source during 1997-2005 ) to a small sink (during 2005-2012). However, the measurements over the last decade (2013 - 2020) indicate a highly interannually varying source/sink. No major trends are found and signals of climate warming or  $\text{CO}_2$  fertilization of NEE, GPP,  $R_{\text{eco}}$  are not immediately evident, though some are present in the driver sensitivities.

At the stand scale, there is little relationship in annual variations in NEE, GPP, or  $R_{\text{eco}}$  between the tall tower and the stand-scale towers, or amongst the stand-scale towers, with the exception of the old-growth forest (US-Syv) and the shrub wetland (US-Los), where a weak positive correlation of NEE ( $r=0.52$ ) is supported by a stronger correlation of GPP ( $r=0.79$ ) over  $R_{\text{eco}}$  ( $r=0.58$ ), suggesting that old-growth forests and wetlands have similar climate sensitivities to photosynthesis. The lack of coherence contrasts with that initially reported within the same study domain by Desai (2010), who reported high correlation among the sites in the first half of the record, connected through phenology and temperature. This finding implies a decoupling of the carbon cycle across the region in the latter decade of observations, perhaps related to differential

responses to a changing climate.

There were also differences in the absolute magnitude of interannual variations in NEE, GPP, and  $R_{eco}$  across the sites. Both forests had consistently higher interannual variability in NEE, partly reflecting the larger magnitude of NEE, but also the greater frequency of disturbances and management. Even after removing years where those effects are prominent, the overall year to year variability in forests still exceeds the wetlands. These variations were more driven by  $R_{eco}$  than GPP, as both absolute and relative variation in  $R_{eco}$  exceeded GPP. Sites had relatively similar interannual variation in GPP with relative variations ranging from 14-18% excluding the shorter-term record of US-ALQ while  $R_{eco}$  variations ranged 15-28%, largest at old-growth forest and the tall tower.

High variation in respiration rates at an old-growth forest is not surprising given greater rates of stand-scale mortality and high soil organic carbon content (Tang *et al.*, 2008). Additionally, enhanced variability in respiration with age is in line with ecological theory describing the successional trajectory of forest NPP (Carey *et al.*, 2001). The high variability of  $R_{eco}$  at the landscape scale is more surprising, as theories of scaling would imply a decrease in temporal variance with an increase in spatial scale for a field that has low spatial correlation, as suggested by the low correlations of interannual variations across the towers. Perhaps this result hints at the important role of shifting patterns in land management, small scale stochastic disturbance events, and climate-sensitive “hot-spots” on the landscape that would be missed by a naive upscaling of the stand-scale towers.

The low interannual variability of carbon fluxes in wetlands had been previously documented (Sulman *et al.*, 2009; Pugh *et al.*, 2018). The relative insensitivity for wetlands appears to be a result of contrasting impacts of water table depth on GPP and  $R_{eco}$ , though the effect works differently in bogs and fens (Sulman *et al.*, 2010). GPP and  $R_{eco}$  variations are strongly correlated and linked to water table, thus canceling out when applied to NEE, except in warm years or extreme water table departures. This effect is consistent with prior experimental studies on northern peatland water table manipulation (Strack & Waddington, 2007)

There are limited related studies on long-term interannual carbon uptake from eddy covariance. The closest is a recent study by Hollinger *et al.* (2021) which evaluated the NEE of the Howland forest (US-Ho1) over a 25 year period. That tower, similar to our forest sites, was a moderate sink of NEE but with smaller interannual variability. Unlike our study, they noted a trend of a slight increase in net carbon uptake despite an increase in climate extremes. Finzi *et al.* (2020) also evaluated a 23-year period of flux measurements at Harvard forest (US-Ha1 and related). Like our network, significant interdecadal variability is present, but unlike our network, this was embedded within a strong trend of a larger carbon sink by 93%. Nearly a third of the interannual variability at this site could be explained by changes in mean annual temperature and growing season

length, especially of increases in red oak biomass and extension of growing season in spring and autumn. Observations of net primary productivity and respiration from additional measurements within the tower footprint confirms the mean magnitude of NEE. The increase in the magnitude of NEE at this site is not smooth, but rather a larger jump from a range around -200 to -300  $\text{gC m}^{-2} \text{ yr}^{-1}$  to one closer to -500  $\text{gC m}^{-2} \text{ yr}^{-1}$ , which Keenan *et al.* (2012) demonstrated is difficult to capture in models and not easily accounted for in carbon stock changes. A recent study from Beringer *et al.* (2022) notes a few long-term ( $> 20$  year) Australian tower sites records, including a temperate mixed Eucalypt forest (AU-Tum) and a tropical savanna (AU-How). These sites experienced increasing water use efficiency with time in response to rising  $\text{CO}_2$  and significant resilience in carbon uptake post-disturbance.

This sense of decadal “breakpoints” in long-term NEE found at US-Ha1 and also noted in our record of US-PFa is further confirmed in Foken *et al.* (2021), which considered several long-running (minimum 20 years) eddy covariance sites in Europe (FI-Hyy, DE-Hai, De-Bay) in addition to US-Ha1. That manuscript noted that abrupt or step changes in annual fluxes were common and linked to potential “regime transitions” associated with step changes in drivers, pointing to the non-smooth trends typical in climate change outside  $\text{CO}_2$ , such as the reported regime shift in the 1980s related to cascading effects from episodic events like volcanic eruptions (Reid *et al.*, 2015). For some sites, like FI-Hyy, these step changes were occurring within a longer-term trend of larger (more negative) NEE from increasing GPP partially promoted by a forest thinning event (Launiainen *et al.*, 2022). Likewise, we saw a relatively large response in enhancement of uptake from thinning of US-WCr in 2013-2014, though that effect weakened after several years. Clear  $\text{CO}_2$  fertilization effects were difficult to delineate in all studies despite those inferred from earlier syntheses of mostly shorter-term flux towers (Chen *et al.*, 2022) or through incorporation of leaf-level findings into global models (e.g., Haverd *et al.*, 2020).

## 4.2 An intriguing role for leaf phenology

While carbon flux variations and trends lack a consistent picture across the sites, there was more coordination among phenology. As with many biological processes, the timing of phenological events is generally accepted to be a function of temperature (Badeck *et al.*, 2004; Schwieger *et al.*, 2019), though recent studies also point to a role of precipitation (Wang *et al.*, 2022). With temperatures increasing globally in response to enhanced atmospheric radiative forcing (IPCC, 2021), it follows that growing seasons would be extended and phenophases such as spring leaf emergence would occur earlier in the year, as winters become milder and spring is ushered in more quickly (Badeck *et al.*, 2004; Menzel *et al.*, 2006; Piao *et al.*, 2015; Polgar & Primack, 2011). Although the magnitude of the trend varies depending on tree species and location, temperate trees are on average experiencing an advancement of spring phenology of 2-8 days/ $^{\circ}\text{C}$  of warming (Menzel *et al.*, 2006; Piao *et al.*, 2015; Richardson *et*

*al.*, 2013; Thompson & Clark, 2008; Walther *et al.*, 2002).

However, while this trend is observed in many places across the globe, it is by no means ubiquitous. Surprisingly, the PhenoCam observations of vegetation deciduous greenness at our sites suggests that growing season length is decreasing at all three sites examined in this study (US-WCr, US-Los, US-Syv), with an average shortening of 4.1 days since the earliest phenocam record in 2012. The observed growing season shortening is predominantly driven by spring leaf out occurring at a later date, with an average yearly shift of 2.63 days. We did not find a direct link of growing season length to annual carbon uptake. Instead, it appears that climate warming factors indirectly influence phenology and carbon uptake, perhaps in a counterintuitive way.

Two factors we found potentially driving this observed divergence from global phenological trends are declining annual snowfall and warmer than average autumn air temperatures. Reduced snowpack depth due to declining annual snowfall diminishes the insulative properties of snow cover, leading to a reduction in spring soil temperatures. Snow serves as an insulating barrier between the underlying soil surface and the atmosphere, buffering soil temperatures from temporary fluctuations in air temperature and reducing heat loss to the surrounding atmosphere through upward conduction from the warmer soil below (Cohen & Rind, 1991). The insulative properties of snow are highly variable depending on snowpack thickness, but soil temperatures generally increase with increasing snow depth (Ge & Gong, 2010). Spring snow cover has been declining in the Northern Hemisphere since the 1950's, a trend that is expected to continue under further warming (IPCC, 2021).

Within the study domain, mean total snowfall decreased by 43% from the first 10 years to the last 10 years of the record. Decreasing snowpack thickness and thus reduced thermal insulation has had a cooling effect on spring soil temperatures across all four measurement depths (2 cm, 5 cm, 10 cm, and 30 cm) at US-WCr, with the most substantial cooling observed closest to the soil surface at a depth of 2 cm. The reduction in spring soil temperatures could impact the timing of spring phenology. The snow effect is explained by interactions between plant phenology, soil moisture, and soil temperature (Piao *et al.*, 2019a). Snow begins to melt in early spring, when soil temperatures are higher than air temperatures on average. The early season moisture supplied by snowmelt percolates down into the layers of soil below, stimulating soil microbial activity and triggering root phenology (Yun *et al.*, 2018). Decreased soil temperature in response to reduced insulation has the potential to result in less active winter and early spring soil microbial communities (Cooper *et al.*, 2011), decreased soil respiration (Morgner *et al.*, 2010) and fine root production (Schwieger *et al.*, 2019), and a muted spring phenological signal, contributing to a delayed onset of spring leaf emergence, and delaying productivity, as has been shown in winter wheat (Zhu *et al.*, 2022). However, the synchrony of physiological coupling between below and above ground phenology are poorly understood, as few phenological studies have paired observations of root phenology with obser-

vations of above ground phenological processes (Piao *et al.*, 2019a, Schwieger *et al.*, 2019). The effect of photoperiod due to cloudier springs can also not be entirely ruled out, thus further analysis is needed.

In addition to snowfall reductions in winter, we note that average seasonal air temperatures increased from 1997-2020 across all four seasons, with the most substantial increase for  $T_{\text{air}}$  observed in autumn. Warmer spring temperatures often lead to earlier spring leaf emergence, but warmer temperatures in autumn and the subsequent shortening of winter can have the opposite effect in high latitude temperate regions, delaying spring leaf out (Beil *et al.*, 2021; Heide, 2003; Roberts *et al.*, 2015). Trees have biological controls on flushing to ensure that leaves flush at the correct time, regardless of temporary fluctuations in air temperature. Part of this control system is the dormancy period, where buds formed towards the end of summer remain in a shallow paradormancy before transitioning to a deep endodormant state through fall senescence and winter (Sutinen *et al.*, 2009). To end this dormancy period, temperatures must be maintained below a certain level for a duration of time, referred to as the chilling period (Piao *et al.*, 2015; Polgar *et al.*, 2014), before sustained warmer temperatures in the spring can trigger dormancy release (Polgar & Primack, 2011; Sutinen *et al.*, 2009). Insufficient chilling during the dormancy period due to warmer temperatures during winter and autumn can delay dormancy release (Yun *et al.*, 2018). Warmer than average fall temperatures can also delay the establishment of bud dormancy (Beil *et al.*, 2021), which typically occurs between September and October in temperate regions. Temperate tree species are highly sensitive to thermal forcing in the spring that determines leafing and flowering, and some temperate species have a commensurate sensitivity to chilling. Vernal wetland and European tree species such as birch, maple, oak, and ash are particularly responsive to temperatures during the preceding fall (Roberts *et al.*, 2015), and are abundant within the study domain.

The shifts in phenological trends presented here represent a reporting of general observations and should be evaluated with caution considering the relatively short phenological data records. Interannual variability in the timing of phenological events is generally large, especially in temperate regions due to the dependence of phenology on highly variable climatic factors such as air temperature (Badeck *et al.*, 2004). Considering this, formal statistical trend analyses of phenological time series need to be conducted across timescales longer than ten years due to the strong correlation between time series length and trend estimates, which can produce misleading results (Post *et al.*, 2018).

### 4.3 Drivers of long-term landscape C variation

Surprisingly, we found a strong role for winter precipitation over growing season climatic variables on interannual variability of NEE, though similar findings were shown for Harvard Forest by Barford *et al.* (2001). Greater winter precipitation increased NEE (made it more positive), which was likely due to an increase in  $R_{\text{eco}}$  in response to greater moisture availability. We found similar trends

in  $R_{10}$ ,  $Q_{10}$  and  $R_d$ , which all increased with greater precipitation, particularly when temperatures were below 0 °C, thus linked to snow accumulation. The increase in  $Q_{10}$  and  $R_d$  resulted in greater ecosystem respiration, particularly during the non-growing season (Fig. 9). Similar to what other studies found (Wang *et al.*, 2011), annual average  $R_{10}$  increased with lower non-growing season temperatures. While the declining trend in NGS temperature was not significant, we observed an increase in temperature extremes in the growing and non-growing season, which could affect site variability directly, via controlling physiological parameters and enzymatic activity, and indirectly by altering moisture availability due to changes in snow and rainfall (Fig. 2). For example, changes in water availability can affect resource reallocation and redistribution of primary and secondary metabolites within plants, particularly during leaf out (Rosell *et al.*, 2020; Tixier *et al.*, 2019), which in turn may lead to reduced growing season lengths.

For GPP, we counterintuitively found increases with greater VPD, which was likely a function of changes in atmospheric moisture demand driving greater transpiration (via greater LE) and stomatal conductance at these sites, consistent with findings of Desai (2014) for US-PFa and with covarying increase in  $R_g$  and PAR consistent with earlier reports of strong control of interannual variability by a small number of beneficial days during the growing season for productivity (Zscheischler *et al.*, 2016). Because we only found a significant increase in  $A_{max}$  with VPD at two out of the five sites, as well as no significant effect of environmental variables on  $\sigma$ , we suspect that passive thermodynamic gradients via greater stomatal conductance (transpiration) resulted in greater GPP at most sites, though the covarying effect of increase PAR with greater VPD cannot be ruled out as a contributing factor. Furthermore, we found that  $\sigma$  did not significantly affect the intra-annual variability in NEE in contrast to  $A_{max}$ , as a result of CO<sub>2</sub> fertilization, rather than an adaption of the light harvesting complexes on an annual scale (Cardona *et al.*, 2018). Similar results were found for other ecosystems (Zhang *et al.*, 2012). A recent study also confirms that many central US ecosystems’ interannual variability in carbon uptake is driven by plant and soil hydraulics (Zhang *et al.*, 2022). Furthermore, respiration dominated inter- and intra-annual NEE variability across sites, thus offsetting any CO<sub>2</sub> fertilization effect (Bugmann & Bigler, 2011; Yu *et al.*, 2021).

Interestingly,  $\sigma$  was also not affected by environmental parameters and further did not differ by site when  $T_{air}$  was below 3.2 °C (data not shown), indicating a temperature threshold for photosynthetic activity, or average temperatures at which leaf out occurs (Aalto *et al.*, 2015; Donnelly *et al.*, 2019), for the different plant species present at all sites. Similarly,  $A_{max}$  did not increase for temperatures < 7.4 °C, which is similar to temperature limitations of photosynthesis found in other studies (Stettz *et al.*, 2022). For the monthly model, we found a significant increase in  $\sigma$  with temperature, independent of site, suggesting that enzymatic activity (i.e., RuBisCo) increased with greater temperatures (Moore *et al.*, 2021). The annual model also showed that  $\sigma$  was significantly greater at US-WCr and US-Los compared to other sites during the growing season, indicat-



ing greater photosynthetic efficiency per amount of radiation received for sites that were dominated by deciduous broadleaved plant species (Qi *et al.*, 2021).

Many remote sensing products estimate changes in carbon dynamics across the globe based on differences in by different plant functional types (i.e., MOD17; Running *et al.*, 2015; Xiao *et al.*, 2004). Yet, here we show that was largely independent of site and environmental variables, with the exception of  $T_{\text{air}}$ , and further did not significantly drive NEE variability, while  $A_{\text{max}}$  was affected by incoming radiation, as well as VPD. These results suggest that remote sensing GPP and NPP products should incorporate plant physiological parameters that describe maximum photosynthetic capacity, in addition to parameters which describe differences in the relationship of carbon uptake to radiation by plant function types. The discrepancy between remote sensing GPP (i.e., MOD17 and MOD17A2/A3) and eddy covariance estimates (Heinsch *et al.*, 2006; Wang *et al.*, 2020; Zhang *et al.*, 2020) may be a result from the exclusion of physiological parameters that better describe this response to environmental variables.

When it comes to  $R_{\text{eco}}$ , an increase in  $T_{\text{air}}$  increased  $R_{\text{eco}}$ , suggesting higher enzyme activity within plants (Moore *et al.*, 2021), as well as microbes, thereby increasing soil respiration as a function of substrate availability (García-Palacios *et al.*, 2021). We also found a significant decrease in  $Q_{10}$  with VPD at the regional scale (for  $T_{\text{air}} > 2.2$  °C), suggesting water limitations on enzymatic processes (Yan *et al.*, 2019). Furthermore, precipitation significantly increased  $Q_{10}$ , further suggesting greater enzymatic activity because of increased moisture availability. In contrast, on the regional scale,  $Q_{10}$  decreased with greater VPD, which was indicative of a feedback of water limitation on microbial respiration (Yuste *et al.*, 2003).

Somewhat in contrast to what other studies found, we found decreasing trends of average annual  $Q_{10}$  with VPD (Niu *et al.*, 2021), while  $T_{\text{air}}$  was not significant in the model. However, VPD and  $T_{\text{air}}$  were correlated at the annual scale (0.36), which likely resulted in an interactive effect on  $Q_{10}$ . We observed lower  $Q_{10}$  at the wetland sites US-ALQ and US-Los, particularly for low VPD and high  $T_{\text{air}}$ , which can be attributed to water availability, soil type and water table variations in wetlands (Mackay *et al.*, 2007). This effect would dampen the response of  $Q_{10}$  to changes in temperature and VPD (Atkin *et al.*, 2005; Chen *et al.*, 2018; Chen *et al.*, 2020; Miao *et al.*, 2013). We further found  $Q_{10}$  changes with temperature only at the old-growth forest and the regional scale, which could either indicate enzymatic sensitivity of autotrophic respiration at these sites (Schindlbacher *et al.*, 2008), or heterotrophic respiration with increasing temperatures (Wang *et al.*, 2014).

Because we also saw an increase in  $R_d$  with higher temperatures at these sites, we suspect that this was a combined effect of greater photorespiration (Walker *et al.*, 2016), as well as microbial substrate decomposition. US-Syv in particular experienced tree die off in 2017 and 2018, leading to an influx of substrate to the forest soil, which may have resulted in the greater respiration rates that were observed. The sharp decrease in  $R_d$  at US-Syv (and US-PFa) with greater VPD

when  $T_{\text{air}}$  was below  $1.5^{\circ}\text{C}$  suggests a reduction in maintenance respiration of coniferous species as a result of closed leaf stomata and limited carbon supply and redistribution when temperatures were low (Seydel *et al.*, 2022). The negative relationship of  $R_d$  to VPD could also be a consequence of reduced canopy conductance (Bao *et al.*, 2019), driven by the coniferous evergreen species that dominate US-Syv and US-PFa.

Nevertheless, changes in temperature dominated the variability of  $R_d$  at all sites.  $R_d$  increased with VPD when  $T_{\text{air}}$  was below  $1.5^{\circ}\text{C}$  at US-WCr, while temperature showed no effect on  $Q_{10}$  and  $R_d$  at that site. US-WCr is dominated by *A. saccharum*, *T. americana* and *F. pennsylvanica*, which lose their leaves during the dormant season, followed by resource redistribution to leaf out during early spring (Tixier *et al.* 2019). Accordingly, the increase in  $R_d$  in response to VPD for  $T < 1.5^{\circ}\text{C}$  could be a function of the redistribution of non-structural carbohydrates (NSC) during spring leaf out (Rosell *et al.*, 2020; Tixier *et al.*, 2019). Furthermore, *A. saccharum* saplings were shown to acclimate respiration to increases in air temperature, resulting in similar rates of respiration for different warming treatments (Gunderson *et al.*, 2000). This acclimation of respiration could be what we also see here. Additionally, limitations in resource availability (i.e., nitrogen) at that site may dampen its response to changes in temperature (Crous *et al.*, 2017; Terrer *et al.*, 2019; Xu *et al.*, 2020a). Our results also indicate differences in activation temperature optimums, quantified via segmented regression, where we found abrupt changes in  $A_{\text{max}}$  at  $7.5^{\circ}\text{C}$ ,  $Q_{10}$  at  $-2.2^{\circ}\text{C}$ , while  $R_d$  showed an increase at  $1.5^{\circ}\text{C}$ , possibly indicating differences in “activation” thresholds of photosynthesis, as well as microbial and autotrophic respiration.

While the effect of  $\text{CO}_2$  is muted in GPP and NEE, we do note that with an increase in  $\text{CO}_2$  by 10 ppm,  $A_{\text{max}}$  and  $R_d$  increased significantly (by 40% and 45%), which is within the range of what other studies have found as a result of  $\text{CO}_2$  fertilization (Chen *et al.*, 2022; Dusenke *et al.*, 2018). Greater increases in  $R_d$  relative to  $A_{\text{max}}$  indicate light limitations on the photosynthetic efficiency, as well as higher expenses to maintain the Calvin-Benson Cycle, with likely greater production of 2-phosphoglycolate requiring higher rates of redox reactions (and thus  $R_d$ ) (Dusenke *et al.*, 2018). We found similar trends for increases in summer air temperature, which could be an indirect effect of  $\text{CO}_2$  fertilization and rising global temperatures on photosynthetic capacity (Sikma *et al.*, 2019). However, our monthly models did not indicate a significant change in  $A_{\text{max}}$  as a result of changes in temperature, possibly a result of acclimation to global warming (Sperry *et al.*, 2019), thus emphasizing the need to account for climate feedbacks from rising  $\text{CO}_2$  (Kolby Smith *et al.*, 2016). Similar trends were observed for eastern hemlock trees (Wilder & Boyd, 2016), which showed no effect of warming in interaction with rising  $\text{CO}_2$  on photosynthetic parameters.

Similarly, phenological changes interacted with  $A_{\text{max}}$  and  $R_d$ . A 10 day reduction in season length resulted in reductions in  $A_{\text{max}}$  and  $R_d$  by 12% and 18.5%, which is likely an indirect effect of changes in shortwave radiation (particularly during the non-growing season as a result of greater precipitation), reducing the

energy available for photosynthesis (Durand *et al.*, 2021), and/or micrometeorological changes due to altered snow dynamics. Greater reductions in  $R_d$  with decreasing season length may be linked to reductions in leaf area and halting NSC redistribution of broadleaved trees during the non-growing season (Asaadi *et al.*, 2018). Season length and  $CO_2$  described the interannual variability in light-response parameters better ( $A_{max}$  and  $R_d$ ), overriding the influence of environmental drivers like air temperature. We found similar results with the intra-annual models, suggesting that these physiological parameters may be indirectly affected by changes in temperature and VPD (Fu *et al.*, 2022), but that they are modulated by plant species composition, and their photosynthetic capacity and leaf phenology.

For intra-annual NEE, we saw the greatest carbon uptake at US-WCr, which is dominated by *A. saccharum* and *T. americana*, which were shown to have greater canopy transpiration compared to other *A. saccharum* sites (Ewers *et al.* 2007), suggesting lower sensitivity of stomata conductance to environmental variables (Carter & Cavaleri, 2018), possibly also a result of higher stand density. Regional scale NEE (US-PFa) was driven by  $A_{max}$ , as well as high  $R_d$  and  $Q_{10}$  with increasing temperature, which differed by tower sites. US-PFa, likely combined fluxes from a mixture of wetlands such as US-ALQ, which showed limitations in  $A_{max}$  and greater respiration during the non-growing season, and old growth and mature forests like US-Syv and US-WCr which showed greater carbon uptake, but also greater respiration, particularly at US-Syv, which also had greater representation by gymnosperms. Gymnosperms like eastern hemlock trees were shown to have lower transpiration compared to deciduous tree species, showing lower canopy stomatal conductance (Tang *et al.*, 2006), which helps explain reductions in photorespiration ( $R_d$ ) in response to increasing VPD.

$A_{max}$  showed a slight increase with VPD at US-Syv, which may have been driven by greater resilience of these trees to atmospheric dryness as a result of lower stomatal conductance. Furthermore, greater  $A_{max}$  may have been the result of broadleaved understory trees (i.e. *B. alleghaniensis*, *C. caroliniana* and *A. saccharum*), as well as more light availability to the understory as a result of tree die off (Ewers *et al.*, 2007; Parker & Dey, 2008). In contrast, US-WCr showed a significant decline in  $A_{max}$  with increases in VPD, which has been observed in other studies of sugar maple stands when experiencing lower snow inputs (Harrison *et al.*, 2020). No significant change in  $A_{max}$  with changes in VPD for low temperatures was likely a result of a lack of leaves before spring leaf emergence of broadleaved plants at the site. Because VPD only significantly affected  $A_{max}$  at two out of the five sites, this suggests that other controlling factors dominated its variability, which were likely a function of physiological limitations of the different plant species (i.e. chlorophyll content, mesophyll structure, etc. Noda *et al.*, 2021).

We also found that  $A_{max}$  did not change with temperature, while respiration components significantly increased with elevated temperatures. While we saw a large increase in  $Q_{10}$  at all sites for temperatures below 1.5°C, this did not

translate to greater NEE release for the non-growing season. In contrast greater NEE was more correlated to a steeper increase in  $R_d$  during the non-growing season, indicating an increase in maintenance respiration by trees (Tang *et al.*, 2021), as well as the initiation of leaf photosynthesis during leaf emergence of broadleaved trees (Tixier *et al.* 2019). Our results suggest that the greater sensitivity of respiration to temperature may result in further reductions in regional carbon uptake in response to climate change (Tang *et al.*, 2021). If such trends persist, respiration may exceed carbon uptake with greater temperatures which could lead to carbon starvation and greater mortality rates in northern forests (McDowell *et al.*, 2020; McDowell *et al.*, 2022). Nevertheless, the shorter growing season trends and increased carbon uptake that we observed could offset this carbon limitation trend (Zhou, 2020).

#### 4.4 Scaling carbon fluxes to the region

The combination of the tall tower and the stand-scale tower affords us the opportunity to evaluate approaches to scaling site level observations to the landscape. Consistent with earlier efforts (e.g., Desai *et al.*, 2008a), a naive upscaling of sites, even 23 of them in this study during the summer 2019 period, does not add up to the US-PFa tall tower NEE, GPP, or  $R_{eco}$  no matter the assumptions made about what percentage of the landscape each individual tower represents. Only 32% of variations in CHEESEHEAD19 flux towers could be explained by the first-principal component, implying large site level effects. This effect is not limited to this single summer. Even with a sufficiently long time series of observations from the long-term towers, site and landscape-level fluxes are not in agreement.

Several hypotheses have been presented on reasons for this. From the sampling side, this includes a strong role of stand age on net uptake, which was seen in the Desai *et al.* (2008a) study where a 17-tower upscaling noted how tower fluxes scaled with stand age and canopy height, and the undersampling of early successional stands, which can often be large carbon sources (Amiro *et al.*, 2010), documented locally in later unpublished works with short-term towers in recently harvested forests (N. Saliendra, personal communications). Xiao *et al.* (2011) estimated gridded scaled fluxes using a parameter constrained ecosystem model in this region using 17 towers. That study noted significant variation within plant functional type parameters, especially when neglecting stand age. The assumptions that go into such a data assimilation consequently generates a large source of uncertainty for upscaling. Recent work from CHEESEHEAD19 also highlights the legacy of a century of land management leaving behind a significant imprint on stand structure and linkages to carbon and water use efficiency (Murphy *et al.*, 2022).

Another line of thinking on the scaling mismatch relates to the role of aquatic ecosystems, including wetlands, lakes, and streams, which are also undersampled generally across eddy covariance networks (Desai *et al.*, 2015a) and further complicated by lateral transport and emissions (Buffam *et al.*, 2011). The

CHEESEHEAD19 observations across four wetlands in addition to US-Los and US-ALQ suggests that it is unlikely that undersampled wetlands are the problem for CO<sub>2</sub> upscaling, though it may be more likely for methane fluxes (Desai *et al.*, 2015b). While lakes are sources of carbon on average (Buffam *et al.*, 2011), the total contribution and areas of water bodies in the footprint is likely too small to be the dominant drivers.

One thing that is clear in Fig. 7 is that the mismatch of NEE is driven by  $R_{eco}$  over GPP. The stand-scale towers have lower  $R_{eco}$ , which would be consistent with a regional contribution from earlier successional forests and water bodies. The region’s forests are heavily managed for wood products and subject to regular wind-blown disturbances, which may only re-visit a single tower site at low frequency, but when scaled to a regional footprint, may be a common feature.

Looking beyond the site-level to the region, hypotheses have also been presented on potential flux footprint biases from the tall tower. The tower NEE time series is based on a standardized algorithm to combine fluxes from three heights (30, 122, and 396 m) relying on incorporating levels with boundary-layer connectivity to the surface (Berger *et al.*, 2001; Davis *et al.*, 2003). A result of this is that the footprint is highly variable from one hour to the next. In particular, the relatively large clearing around the tower may over-represent the flux measurements especially in the daytime (Xu *et al.*, 2017). Early upscaling work attempted to account for this footprint bias found a larger carbon sink at the tall tower using a variety of “rectification” approaches (e.g., Wang *et al.*, 2006; Desai *et al.*, 2008a), which also made the tall tower fluxes more consistent with upscaling performed with the Ecosystem Demography dynamic vegetation ecosystem model (Desai *et al.*, 2007) and with top-down tracer transport inversions (Desai *et al.*, 2010). Interestingly, footprint biases do not seem to be a significant issue for upscaling either evapotranspiration flux (Mackay *et al.*, 2002) or methane fluxes (Desai, *et al.*, 2015a), though the limited number of measurements in the latter prevents a clear conclusion on that. Challenges in linking tall tower to stand scale fluxes were also noted in a study in Siberia (Winderlich *et al.*, 2014).

Recent attempts to apply more advanced scaling techniques have further supported the importance of footprint-based correction of eddy-covariance flux measurements, especially for heterogeneous footprints (Chu *et al.*, 2021; Metzger *et al.*, 2013; Metzger, 2018; Xu *et al.*, 2017; Xu *et al.*, 2020b). The Environmental Response Function (ERF) approach attempts to attribute individual footprint to component fluxes and drivers from the landscape. For US-PFa, ERF does indicate an over-representation of the clearing around the tower and a significant difference in land cover for nighttime and daytime (Xu *et al.*, 2017). The corrected gridded fluxes from ERF fell closer in line to the stand-scale towers. Nonetheless, hot-spots of fluxes still persist and warrant further consideration for reconciling stand, tall tower, and regional flux estimates.

The findings here do suggest a concentrated effort is required to resolve scaling

mismatches. While some issues may be unique to our study area, top-down and bottom-up differences in estimates of the terrestrial biosphere carbon flux are routine and widespread (Hayes *et al.*, 2012). The global eddy covariance tower network oversamples pristine undistributed or rarely disturbed expansive ecosystems often within protected lands, mature established forests, productive grasslands, and mid-latitude ecosystems, all typically large carbon sinks, while undersampling wetlands and lakes, early successional forests, managed or frequently disturbed systems, land cover transitions and edges, and anthropogenic land covers (Jung *et al.*, 2020). While there have been successful upscaling efforts (e.g., Xiao *et al.*, 2014; Jung *et al.*, 2020), studies using dense networks of towers such as CHEESEHEAD19 and application of advanced scaling approaches provide a future opportunity for refinement and reconciliation.

## 5. Conclusion

Eddy covariance flux towers are a mature technology (Baldocchi, 2020). The growing number of long-term records has challenged our estimation of trends, sensitivities, and models (Foken *et al.*, 2021; Keenan *et al.*, 2012). Insight from tower clusters sampling key gradients or representative ecosystems has helped resolve spatial variation in carbon cycle-climate sensitivity (e.g., Biederman *et al.*, 2017) or regional upscaling (e.g., Xiao *et al.*, 2011). Here, we have the luxury of combining long-term records within a single cluster established by a team of researchers over the past quarter century.

Overall, our findings are not straightforward, and the longer records even challenge findings of earlier studies from co-authors here. Towers that were once highly correlated in interannual variations in NEE, GPP, or  $R_{eco}$ , as reported in Desai (2010), no longer are. An old-growth tower is more related in variation to a fen wetland than a mature forest. A nearly 14% or 50 ppm rise in atmospheric  $CO_2$  appears to have had no clear effect on GPP, though it has affected parameters that determine GPP light-limited assimilation and dark respiration rate, with little change in quantum yield and these results are site specific. Earlier studies pointing to a strong role for atmospheric dryness, despite relative lack of moisture limitation in the region (Desai, 2014), were confirmed but we found the effect more on increasing GPP and on lowering the temperature sensitivity of respiration. Most surprisingly, the earlier end of winter was not extending growing season length, but rather we link the reduced snowpack to reduced soil insulation, delaying the start of leaf out.

Meanwhile, our results also show the limits of simple approaches to upscaling. Nineteen quasi-randomly placed towers within 10 km of the tall tower, along with the other four stand-scale long-term towers, show ranges of NEE that do not add up to the tall tower regional flux regardless of what assumptions are made about land cover fraction or relative representation of sites. Some of this may be in footprint biases from the tall tower, while others may be in the importance of hot-spots and hot-moments in the landscape that contribute disproportionately

to the flux but are difficult to sample with traditional flux tower techniques. Emerging approaches that account for footprint variation and landscape drivers of extreme fluxes (e.g., Xu *et al.*, 2017) are essential to advance scaling fluxes needed for landscape ecology, natural climate solution verification (Novick *et al.*, 2022), and global carbon budgeting and comparisons to top-down estimates (Desai *et al.*, 2010).

Our results also provide some guidance to improving models. There appears to be a common control on photosynthetic light response to VPD, while maximum assimilation rates are limited by CO<sub>2</sub> and moisture availability. Phenology and soil models need to capture the insulation effect of snow on soil temperature and the link of soil temperature on leaf out. Benchmarking of regional fluxes from models or tracer-transport inversions against flux towers needs to consider footprint variability and site biases. No site or region is as homogenous as normally assumed.

The terrestrial biosphere carbon cycle is a highly non-linear and coupled system that leads to extraordinary variance in space and time. Drawing inferences about a region from a single tower for periods of record less than a decade should be done with caution and with appropriate accounting for uncertainty and surprises. Our results and open-access data should be complemented with addition of more networks of long-term co-located sites coupled with ancillary data on composition, phenology, respiration, and physiology. Such efforts will be essential for new insights into landscape carbon-climate coupling and for improving our projections and management of the biosphere in a changing climate.

## Acknowledgements

We acknowledge the work of many dedicated technicians, students, and researchers who worked in constructing, operating, and analyzing instruments and observations from the ChEAS core site cluster, the CHEESEHEAD19 sites, and related sites for the past quarter century. In addition, we acknowledge the support of our land holders, the US Forest Service Chequamegon-Nicolet National Forest and Ottawa National Forest, the State of Wisconsin Dept of Natural Resources, and State of Wisconsin Educational Communications Board. We would like to thank Christina Staudhammer for statistical advice. We also recognize that our field research occurs on the traditional territories of the Ojibwe people, which have been unjustly ceded and whose ancestors were the original scientists and naturalists who stewarded the land, air, and waters we are fortunate to observe, reflect, and hopefully help continue to flourish. Funding agencies that supports the towers include Dept of Energy (DOE) Ameriflux Network Management Project contract to the ChEAS core site cluster, NSF grants #0845166 and #1822420, Wisconsin Focus on Energy, EERD #10-06, USDA North Central Research Station, Department of Energy, NICCR Midwest, 050516Z19, DOE Terrestrial Carbon Processes, and NASA Carbon Cycle. This manuscript was a joint project of the UW Ecometeorology lab members

and collaborators conducted over the pandemic in weekly lab meetings. All authors contributed equally across aspects of conceptualization, data collection, quality control, analysis, visualization, discussion, writing, and editing.

## Open Research

Ameriflux eddy covariance flux observations are all located at the Ameriflux repository at <https://ameriflux.lbl.gov> and specific DOIs noted in Table 1. Additional ancillary metadata and observations for these sites can be found at: <https://flux.aos.wisc.edu/fluxdata> CHEESEHEAD19 observations are archived at [https://www.eol.ucar.edu/field\\_projects/cheesehead](https://www.eol.ucar.edu/field_projects/cheesehead) Phenocam data are archived at <https://phenocam.sr.unh.edu/webcam/> Long-term precipitation observations were acquired from MRCC <https://mrcc.purdue.edu/>

## Works Cited

Aalto, J., Porcar-Castell, A., Atherton, J., Kolari, P., Pohja, T., Hari, P., Nikinmaa, E., Petäjä, T., & Bäck, J. (2015). Onset of photosynthesis in spring speeds up monoterpene synthesis and leads to emission bursts. *Plant, Cell & Environment*, 38(11), 2299–2312. <https://doi.org/10.1111/pce.12550>

Amiro, B. D., Barr, A. G., Barr, J. G., Black, T. A., Bracho, R., Brown, M., Chen, J., Clark, K. L., Davis, K. J., Desai, A. R., Dore, S., Engel, V., Fuentes, J. D., Goldstein, A. H., Goulden, M. L., Kolb, T. E., Lavigne, M. B., Law, B. E., Margolis, H. A., ... Xiao, J. (2010). Ecosystem carbon dioxide fluxes after disturbance in forests of North America. *Journal of Geophysical Research*, 115. <https://doi.org/10.1029/2010jg001390>

Andrews, A. E., Kofler, J. D., Trudeau, M. E., Williams, J. C., Neff, D. H., Masarie, K. A., Chao, D. Y., Kitzis, D. R., Novelli, P. C., Zhao, C. L., Dlugokencky, E. J., Lang, P. M., Crotwell, M. J., Fischer, M. L., Parker, M. J., Lee, J. T., Baumann, D. D., Desai, A. R., Stanier, C. O., ... Tans, P. P. (2014). CO<sub>2</sub>, CO, and CH<sub>4</sub> measurements from tall towers in the NOAA Earth System Research Laboratory’s Global Greenhouse Gas Reference Network: Instrumentation, uncertainty analysis, and recommendations for future high-accuracy greenhouse gas monitoring efforts. *Atmospheric Measurement Techniques*, 7(2), 647–687. <https://doi.org/10.5194/amt-7-647-2014>

Asaadi, A., Arora, V. K., Melton, J. R., & Bartlett, P. (2018). An improved parameterization of Leaf Area index (LAI) seasonality in the Canadian Land Surface scheme (class) and Canadian Terrestrial Ecosystem Model (CTEM) modelling Framework. *Biogeosciences*, 15(22), 6885–6907. <https://doi.org/10.5194/bg-15-6885-2018>

Atkin, O. K., Bruhn, D., Hurry, V. M., & Tjoelker, M. G. (2005). The hot and the cold: Unravelling the variable response of plant respiration to temperature.



*Functional Plant Biology*, 32(2), 87. <https://doi.org/10.1071/fp03176>

Badeck, F. W., Bondeau, A., Böttcher, K., Doktor, D., Lucht, W., Schaber, J., & Sitch, S. (2004). Responses of spring phenology to climate change. *New Phytologist*, 162(2), 295–309. <https://doi.org/10.1111/j.1469-8137.2004.01059.x>

Bakwin, P. S., Tans, P. P., Hurst, D. F., & Zhao, C. (1998). Measurements of carbon dioxide on very tall towers: Results of the NOAA/CMDL program. *Tellus B: Chemical and Physical Meteorology*, 50(5), 401–415. <https://doi.org/10.3402/tellusb.v50i5.16216>

Baldocchi, D. D. (2014). Measuring fluxes of trace gases and energy between ecosystems and the atmosphere - the state and future of the Eddy Covariance Method. *Global Change Biology*, 20(12), 3600–3609. <https://doi.org/10.1111/gcb.12649>

Baldocchi, D. D. (2020). How eddy covariance flux measurements have contributed to our understanding of Global Change Biology. *Global Change Biology*, 26(1), 242–260. <https://doi.org/10.1111/gcb.14807>

Baldocchi, D. D., Chu, H., & Reichstein, M. (2018). Inter-annual variability of net and gross ecosystem carbon fluxes: A review. *Agricultural and Forest Meteorology*, 249, 520–533. <https://doi.org/10.1016/j.agrformet.2017.05.015>

Ballantyne, A. P., Liu, Z., Anderegg, W. R. L., Yu, Z., Stoy, P., & Poulter, B. (2021). Reconciling carbon-cycle processes from ecosystem to global scales. *Frontiers in Ecology and the Environment*, 19(1), 57–65. <https://doi.org/10.1002/fee.2296>.

Bao, X., Li, Z., & Xie, F. (2019). Environmental influences on light response parameters of net carbon exchange in two rotation croplands on the North China Plain. *Scientific Reports*, 9(1). <https://doi.org/10.1038/s41598-019-55340-2>

Barford C.C., Wofsy S.C., Goulden M.L., Munger J.W., Pyle E.H., Urbanski S.P., Hutya L., Saleska S.R., Fitzjarrald D., Moore K (2001). Factors controlling long- and short-term sequestration of atmospheric CO<sub>2</sub> in a mid-latitude forest. *Science*, 294, 1688–91. <https://doi.org/10.1126/science.1062962>.

Beil, I., Kreyling, J., Meyer, C., Lemcke, N., & Malyshev, A. V. (2021). Late to bed, late to rise—warmer autumn temperatures delay spring phenology by delaying dormancy. *Global Change Biology*, 27(22), 5806–5817. <https://doi.org/10.1111/gcb.15858>

Benson, Barbara J., Timothy K. Kratz, and John J. Magnuson. (2006). Long-term dynamics of lakes in the landscape: long-term ecological research on north temperate lakes. Oxford University Press on Demand.

Berger, B. W., Davis, K. J., Yi, C., Bakwin, P. S., & Zhao, C. L. (2001). Long-term carbon dioxide fluxes from a very tall tower in a northern forest: Flux measurement methodology. *Journal of Atmospheric and Oceanic Technology*, 18(4), 529–542. [https://doi.org/10.1175/1520-0426\(2001\)018%3C0529:LTCDFF%3E2.0.CO;2](https://doi.org/10.1175/1520-0426(2001)018%3C0529:LTCDFF%3E2.0.CO;2)

Beringer, J., Moore, C. E., Cleverly, J., Campbell, D. I., Cleugh, H., *et al.* (2022). Bridge to the future: Important lessons from 20 years of ecosystem observations made by the OzFlux network. *Global Change Biology*, 28, 3489–3514. <https://doi.org/10.1111/gcb.16141>

Biederman, J. A., Scott, R. L., Bell, T. W., Bowling, D. R., Dore, S., Garatuza-Payan, J., Kolb, T. E., Krishnan, P., Krofcheck, D. J., Litvak, M. E., Maurer, G. E., Meyers, T. P., Oechel, W. C., Papuga, S. A., Ponce-Campos, G. E., Rodriguez, J. C., Smith, W. K., Vargas, R., Watts, C. J., ... Goulden, M. L. (2017). CO<sub>2</sub> exchange and evapotranspiration across dryland ecosystems of southwestern North America. *Global Change Biology*, 23(10), 4204–4221. <https://doi.org/10.1111/gcb.13686>

Briegel, F., Lee, S. C., Black, T. A., Jassal, R. S., & Christen, A. (2020). Factors controlling long-term carbon dioxide exchange between a Douglas-fir stand and the atmosphere identified using an artificial neural network approach. *Ecological Modelling*, 435, 109266. <https://doi.org/10.1016/j.ecolmodel.2020.109266>

Buffam, I., Turner, M. G., Desai, A. R., Hanson, P. C., Rusak, J. A., Lotig, N. R., Stanley, E. H., & Carpenter, S. R. (2011). Integrating aquatic and terrestrial components to construct a complete carbon budget for a north temperate lake district. *Global Change Biology*, 17(2), 1193–1211. <https://doi.org/10.1111/j.1365-2486.2010.02313.x>

Bugmann, H., & Bigler, C. (2011). Will the CO<sub>2</sub> fertilization effect in forests be offset by reduced tree longevity? *Oecologia*, 165(2), 533–544. <https://doi.org/10.1007/s00442-010-1837-4>

Burba, G. (2019, August 6). Illustrative maps of past and present Eddy Covariance measurement locations: II. High-resolution images. ResearchGate. Retrieved May 3, 2022, from [https://www.researchgate.net/publication/335004533\\_Illustrative\\_Maps\\_of\\_Past](https://www.researchgate.net/publication/335004533_Illustrative_Maps_of_Past)

Butterworth, B. J., Desai, A. R., Townsend, P. A., Petty, G. W., Andresen, C. G., Bertram, T. H., Kruger, E. L., Mineau, J. K., Olson, E. R., Paleri, S., Pertzborn, R. A., Pettersen, C., Stoy, P. C., Thom, J. E., Vermeuel, M. P., Wagner, T. J., Wright, D. B., Zheng, T., Metzger, S., ... Wilczak, J. M. (2021). Connecting land–atmosphere interactions to surface heterogeneity in CHEESEHEAD19. *Bulletin of the American Meteorological Society*, 102(2), E421–E445. <https://doi.org/10.1175/bams-d-19-0346.1>

Cardona, T., Shao, S., & Nixon, P. J. (2018). Enhancing photosynthesis in plants: The light reactions. *Essays in Biochemistry*, 62(1), 85–94. <https://doi.org/10.1042/ebc20170015>

Carey, E. V., Sala, A., Keane, R., & Callaway, R. M. (2001). Are old forests underestimated as global carbon sinks? *Global Change Biology*, 7(4), 339–344. <https://doi.org/10.1046/j.1365-2486.2001.00418.x>

Carter, K. R., & Cavaleri, M. A. (2018). Within-canopy experimental leaf warming induces photosynthetic decline instead of acclimation in two

- northern hardwood species. *Frontiers in Forests and Global Change*, 1. <https://doi.org/10.3389/ffgc.2018.00011>
- Chen, C., Riley, W. J., Prentice, I. C., & Keenan, T. F. (2022). CO<sub>2</sub> fertilization of terrestrial photosynthesis inferred from site to global scales. *Proceedings of the National Academy of Sciences*, 119(10). <https://doi.org/10.1073/pnas.2115627119>
- Chen, H., Zou, J., Cui, J., Nie, M., & Fang, C. (2018). Wetland drying increases the temperature sensitivity of soil respiration. *Soil Biology and Biochemistry*, 120, 24–27. <https://doi.org/10.1016/j.soilbio.2018.01.035>
- Chen, S., Wang, J., Zhang, T., & Hu, Z. (2020). Climatic, soil, and vegetation controls of the temperature sensitivity (Q<sub>10</sub>) of soil respiration across terrestrial biomes. *Global Ecology and Conservation*, 22. <https://doi.org/10.1016/j.gecco.2020.e00955>
- Chu, H., Luo, X., Ouyang, Z., Chan, W. S., Dengel, S., Biraud, S. C., Torn, M. S., Metzger, S., Kumar, J., Arain, M. A., Arkebauer, T. J., Baldocchi, D., Bernacchi, C., Billesbach, D., Black, T. A., Blanken, P. D., Bohrer, G., Bracho, R., Brown, S., ... Zona, D. (2021). Representativeness of eddy-covariance flux footprints for areas surrounding Ameriflux Sites. *Agricultural and Forest Meteorology*, 301–302, 108350. <https://doi.org/10.1016/j.agrformet.2021.108350>
- Cohen, J., & Rind, D. (1991). The effect of snow cover on the climate. *Journal of Climate*, 4(7), 689–706. [https://doi.org/10.1175/1520-0442\(1991\)004<0689:TEOSCO>2.0.CO;2](https://doi.org/10.1175/1520-0442(1991)004<0689:TEOSCO>2.0.CO;2)
- Cook, B. D., Bolstad, P. V., Martin, J. G., Heinsch, F. A., Davis, K. J., Wang, W., Desai, A. R., & Teclaw, R. M. (2008). Using light-use and production efficiency models to predict photosynthesis and net carbon exchange during Forest Canopy Disturbance. *Ecosystems*, 11(1), 26–44. <https://doi.org/10.1007/s10021-007-9105-0>
- Cook, B. D., Davis, K. J., Wang, W., Desai, A., Berger, B. W., Teclaw, R. M., Martin, J. G., Bolstad, P. V., Bakwin, P. S., Yi, C., & Heilman, W. (2004). Carbon exchange and venting anomalies in an upland deciduous forest in northern Wisconsin, USA. *Agricultural and Forest Meteorology*, 126(3–4), 271–295. <https://doi.org/10.1016/j.agrformet.2004.06.008>
- Cooper, E. J., Dullinger, S., & Semenchuk, P. (2011). Late snowmelt delays plant development and results in lower reproductive success in the High Arctic. *Plant Science*, 180(1), 157–167. <https://doi.org/10.1016/j.plantsci.2010.09.005>
- Cox, D. T., Maclean, I. M., Gardner, A. S., & Gaston, K. J. (2020). Global variation in diurnal asymmetry in temperature, cloud cover, specific humidity and precipitation and its association with Leaf Area Index. *Global Change Biology*, 26(12), 7099–7111. <https://doi.org/10.1111/gcb.15336>
- Creswell, J. E., Kerr, S. C., Meyer, M. H., Babiarz, C. L., Shafer, M. M., Armstrong, D. E., & Roden, E. E. (2008). Factors controlling temporal and spatial distribution of total mercury and methylmercury in hyporheic sediments

- of the Allequash Creek Wetland, northern Wisconsin. *Journal of Geophysical Research: Biogeosciences*, 113(G2). <https://doi.org/10.1029/2008jg000742>
- Crous, K. Y., Wallin, G., Atkin, O. K., Uddling, J., & af Ekenstam, A. (2017). Acclimation of light and dark respiration to experimental and seasonal warming are mediated by changes in leaf nitrogen in eucalyptus globulus. *Tree Physiology*, 37(8), 1069–1083. <https://doi.org/10.1093/treephys/tpx052>
- Davis, K. J., Bakwin, P. S., Yi, C., Berger, B. W., Zhao, C., Teclaw, R. M., & Isebrands, J. G. (2003). The annual cycles of CO<sub>2</sub> and H<sub>2</sub>O exchange over a northern mixed forest as observed from a very tall tower. *Global Change Biology*, 9(9), 1278–1293. <https://doi.org/10.1046/j.1365-2486.2003.00672.x>
- Desai, A. R. (2010). Climatic and phenological controls on coherent regional interannual variability of carbon dioxide flux in a heterogeneous landscape. *Journal of Geophysical Research*, 115(G3). <https://doi.org/10.1029/2010jg001423>
- Desai, A. R. (2014). Influence and predictive capacity of climate anomalies on daily to decadal extremes in canopy photosynthesis. *Photosynthesis Research*, 119(1-2), 31–47. <https://doi.org/10.1007/s1120-013-9925-z>
- Desai, A. R., Bolstad, P. V., Cook, B. D., Davis, K. J., & Carey, E. V. (2005). Comparing net ecosystem exchange of carbon dioxide between an old-growth and mature forest in the Upper Midwest, USA. *Agricultural and Forest Meteorology*, 128(1-2), 33–55. <https://doi.org/10.1016/j.agrformet.2004.09.005>
- Desai, A. R., Moorcroft, P. R., Bolstad, P. V., & Davis, K. J. (2007). Regional carbon fluxes from an observationally constrained dynamic ecosystem model: Impacts of disturbance, CO<sub>2</sub> fertilization, and heterogeneous land cover. *Journal of Geophysical Research*, 112(G1). <https://doi.org/10.1029/2006jg000264>
- Desai, A. R., Noormets, A., Bolstad, P. V., Chen, J., Cook, B. D., Davis, K. J., Euskirchen, E. S., Gough, C., Martin, J. G., Ricciuto, D. M., Schmid, H. P., Tang, J., & Wang, W. (2008a). Influence of vegetation and seasonal forcing on carbon dioxide fluxes across the Upper Midwest, USA: Implications for regional scaling. *Agricultural and Forest Meteorology*, 148(2), 288–308. <https://doi.org/10.1016/j.agrformet.2007.08.001>
- Desai, A. R., Richardson, A. D., Moffat, A. M., Kattge, J., Hollinger, D. Y., Barr, A., Falge, E., Noormets, A., Papale, D., Reichstein, M., & Stauch, V. J. (2008b). Cross-site evaluation of eddy covariance GPP and RE Decomposition Techniques. *Agricultural and Forest Meteorology*, 148(6-7), 821–838. <https://doi.org/10.1016/j.agrformet.2007.11.012>
- Desai, A. R., Helliker, B. R., Moorcroft, P. R., Andrews, A. E., & Berry, J. A. (2010). Climatic controls of interannual variability in regional carbon fluxes from top-down and bottom-up perspectives. *Journal of Geophysical Research: Biogeosciences*, 115(G2). <https://doi.org/10.1029/2009jg001122>
- Desai, A. R., Vesala, T., & Rantakari, M. (2015a). Measurements, modeling, and scaling of inland water gas exchange. *Eos*, 96. <https://doi.org/10.1029/2015eo022151>

Desai, A. R., Xu, K., Tian, H., Weishampel, P., Thom, J., Baumann, D., Andrews, A. E., Cook, B. D., King, J. Y., & Kolka, R. (2015b). Landscape-level terrestrial methane flux observed from a very tall tower. *Agricultural and Forest Meteorology*, 201, 61–75. <https://doi.org/10.1016/j.agrformet.2014.10.017>

Desai, A. R., Khan, A. M., Zheng, T., Paleri, S., Butterworth, B., Lee, T. R., Fisher, J. B., Hulley, G., Kleynhans, T., Gerace, A., Townsend, P. A., Stoy, P., & Metzger, S. (2021). Multi-sensor approach for high space and time resolution land surface temperature. *Earth and Space Science*, 8(10). <https://doi.org/10.1029/2021ea001842>

Durand, M., Murchie, E. H., Lindfors, A. V., Urban, O., Aphalo, P. J., & Robson, T. M. (2021). Diffuse solar radiation and canopy photosynthesis in a changing environment. *Agricultural and Forest Meteorology*, 311, 108684. <https://doi.org/10.1016/j.agrformet.2021.108684>

Donnelly, A., Yu, R., Liu, L., Hanes, J.M., Liang, L., Schwartz, M. Desai, A.R. (2019). Comparing in-situ leaf observations in early spring with flux tower CO<sub>2</sub> exchange and MODIS EVI in a northern mixed forest. *Ag. Forest Meteorol.*, 278, 107673. <https://doi.org/10.1016/j.agrformet.2019.107673>.

Dusenge, M. E., Duarte, A. G., & Way, D. A. (2018). Plant Carbon Metabolism and climate change: Elevated CO<sub>2</sub> and temperature impacts on photosynthesis, photorespiration and respiration. *New Phytologist*, 221(1), 32–49. <https://doi.org/10.1111/nph.15283>

Ewers, B. E., Mackay, D. S., & Samanta, S. (2007). Interannual consistency in canopy stomatal conductance control of leaf water potential across seven tree species. *Tree Physiology*, 27(1), 11–24. <https://doi.org/10.1093/treephys/27.1.11>

Finzi, A. C., Giasson, M. A., Barker Plotkin, A. A., Aber, J. D., Boose, E. R., Davidson, E. A., Dietze, M. C., Ellison, A. M., Frey, S. D., Goldman, E., Keenan, T. F., Melillo, J. M., Munger, J. W., Nadelhoffer, K. J., Ollinger, S. V., Orwig, D. A., Pederson, N., Richardson, A. D., Savage, K., ... Foster, D. R. (2020). Carbon budget of the Harvard Forest long-term ecological research site: Pattern, process, and response to global change. *Ecological Monographs*, 90(4). <https://doi.org/10.1002/ecm.1423>

Fisher, J. B., Melton, F., Middleton, E., Hain, C., Anderson, M., Allen, R., McCabe, M. F., Hook, S., Baldocchi, D., Townsend, P. A., Kilic, A., Tu, K., Miralles, D. D., Perret, J., Lagouarde, J.-P., Waliser, D., Purdy, A. J., French, A., Schimel, D., ... Wood, E. F. (2017). The future of evapotranspiration: Global requirements for ecosystem functioning, carbon and climate feedbacks, agricultural management, and water resources. *Water Resources Research*, 53(4), 2618–2626. <https://doi.org/10.1002/2016wr020175>

Foken, T., Babel, W., Munger, J. W., Grönholm, T., Vesala, T., & Knohl, A. (2021). Selected breakpoints of net forest carbon uptake at four eddy-covariance sites. *Tellus B: Chemical and Physical Meteorology*, 73(1), 1–12. <https://doi.org/10.1080/16000889.2021.1915648>

- Friedlingstein, P., Cox, P., Betts, R., Bopp, L., von Bloh, W., Brovkin, V., Cadule, P., Doney, S., Eby, M., Fung, I., Bala, G., John, J., Jones, C., Joos, F., Kato, T., Kawamiya, M., Knorr, W., Lindsay, K., Matthews, H. D., ... Zeng, N. (2006). Climate-carbon cycle feedback analysis: Results from the C4MIP model intercomparison. *Journal of Climate*, 19(14), 3337–3353. <https://doi.org/10.1175/jcli3800.1>
- Friedlingstein, P., O’Sullivan, M., Jones, M. W., Andrew, R. M., Hauck, J., Olsen, A., Peters, G. P., Peters, W., Pongratz, J., Sitch, S., Le Quéré, C., Canadell, J. G., Ciais, P., Jackson, R. B., Alin, S., Aragão, L. E., Arneeth, A., Arora, V., Bates, N. R., ... Zaehle, S. (2020). Global carbon budget 2020. *Earth System Science Data*, 12(4), 3269–3340. <https://doi.org/10.5194/essd-12-3269-2020>
- Fu, Z., Stoy, P. C., Poulter, B., Gerken, T., Zhang, Z., Wakbulcho, G., & Niu, S. (2019). Maximum carbon uptake rate dominates the interannual variability of global net ecosystem exchange. *Global Change Biology*, 25(10), 3381–3394. <https://doi.org/10.1111/gcb.14731>
- Fu, Z., Ciais, P., Prentice, I. C., Gentine, P., Makowski, D., Bastos, A., Luo, X., Green, J. K., Stoy, P. C., Yang, H., & Hajima, T. (2022). Atmospheric dryness reduces photosynthesis along a large range of soil water deficits. *Nature Communications*, 13(1). <https://doi.org/10.1038/s41467-022-28652-7>
- García-Palacios, P., Crowther, T. W., Dacal, M., Hartley, I. P., Reinsch, S., Rinnan, R., Rousk, J., van den Hoogen, J., Ye, J.-S., & Bradford, M. A. (2021). Evidence for large microbial-mediated losses of soil carbon under anthropogenic warming. *Nature Reviews Earth & Environment*, 2(7), 507–517. <https://doi.org/10.1038/s43017-021-00178-4>
- Ge, Y., & Gong, G. (2010). Land surface insulation response to snow depth variability. *Journal of Geophysical Research*, 115(D8). <https://doi.org/10.1029/2009jd012798>
- Gorsky, A. L., Lottig, N. R., Stoy, P. C., Desai, A. R., & Dugan, H. A. (2021). The importance of spring mixing in evaluating carbon dioxide and methane flux from a small north-temperate Lake in Wisconsin, United States. *Journal of Geophysical Research: Biogeosciences*, 126(12). <https://doi.org/10.1029/2021jg006537>
- Gough, Robert J. (1997) *Farming the cutover: A social history of northern Wisconsin, 1900-1940*. University Press of Kansas.
- Grimm, N. B., Chapin, F. S., Bierwagen, B., Gonzalez, P., Groffman, P. M., Luo, Y., Melton, F., Nadelhoffer, K., Pairis, A., Raymond, P. A., Schimel, J., & Williamson, C. E. (2013). The impacts of climate change on ecosystem structure and function. *Frontiers in Ecology and the Environment*, 11(9), 474–482. <https://doi.org/10.1890/120282>
- Grossiord, C., Buckley, T. N., Cernusak, L. A., Novick, K. A., Poulter, B., Siegwolf, R. T., Sperry, J. S., & McDowell, N. G. (2020). Plant re-

sponses to rising vapor pressure deficit. *New Phytologist*, 226(6), 1550–1566. <https://doi.org/10.1111/nph.16485>

Gunderson, C. A., Norby, R. J., & Wullschleger, S. D. (2000). Acclimation of photosynthesis and respiration to simulated climatic warming in northern and southern populations of *Acer saccharum*: Laboratory and field evidence. *Tree Physiology*, 20(2), 87–96. <https://doi.org/10.1093/treephys/20.2.87>

Harrison, J. L., Reinmann, A. B., Maloney, A. S., Phillips, N., Juice, S. M., Webster, A. J., & Templer, P. H. (2020). Transpiration of dominant tree species varies in response to projected changes in climate: Implications for composition and water balance of temperate forest ecosystems. *Ecosystems*, 23(8), 1598–1613. <https://doi.org/10.1007/s10021-020-00490-y>

Haverd, V., Smith, B., Canadell, J. G., Cuntz, M., Mikaloff-Fletcher, S., Farquhar, G., Woodgate, W., Briggs, P. R., & Trudinger, C. M. (2020). Higher than expected CO<sub>2</sub> fertilization inferred from leaf to global observations. *Global Change Biology*, 26(4), 2390–2402. <https://doi.org/10.1111/gcb.14950>

Hayes, D. J., Turner, D. P., Stinson, G., McGuire, A. D., Wei, Y., West, T. O., Heath, L. S., Jong, B., McConkey, B. G., Birdsey, R. A., Kurz, W. A., Jacobson, A. R., Huntzinger, D. N., Pan, Y., Post, W. M., & Cook, R. B. (2012). Reconciling estimates of the contemporary North American carbon balance among terrestrial biosphere models, atmospheric inversions, and a new approach for estimating net ecosystem exchange from inventory-based data. *Global Change Biology*, 18(4), 1282–1299. <https://doi.org/10.1111/j.1365-2486.2011.02627.x>

Heide, O. M. (2003). High autumn temperature delays spring bud burst in boreal trees, counterbalancing the effect of climatic warming. *Tree Physiology*, 23(13), 931–936. <https://doi.org/10.1093/treephys/23.13.931>

Heinsch, F. A., Zhao, M., Running, S. W., Kimball, J. S., Nemani, R. R., Davis, K. J., Bolstad, P. V., Cook, B. D., Desai, A. R., Ricciuto, D. M., Law, B. E., Oechel, W. C., Kwon, H., Luo, H., Wofsy, S. C., Dunn, A. L., Munger, J. W., Baldocchi, D. D., Xu, L., ... Flanagan, L. B. (2006). Evaluation of remote sensing based terrestrial productivity from Modis using regional tower eddy flux network observations. *IEEE Transactions on Geoscience and Remote Sensing*, 44(7), 1908–1925. <https://doi.org/10.1109/tgrs.2005.853936>

Hollinger, D. Y., Davidson, E. A., Fraver, S., Hughes, H., Lee, J. T., Richardson, A. D., Savage, K., Sihi, D., & Teets, A. (2021). Multi-decadal carbon cycle measurements indicate resistance to external drivers of change at the Howland Forest Ameriflux Site. *Journal of Geophysical Research: Biogeosciences*, 126(8). <https://doi.org/10.1029/2021jg006276>

Humphrey, V., Berg, A., Ciais, P., Gentile, P., Jung, M., Reichstein, M., Seneviratne, S. I., & Frankenberg, C. (2021). Soil moisture–atmosphere feedback dominates land carbon uptake variability. *Nature*, 592(7852), 65–69. <https://doi.org/10.1038/s41586-021-03325-5>

IPCC. (2021). *Climate change 2021 - The Physical Science Basis. Contribution of Working Group I to the Sixth Assessment Report of the Intergovernmental Panel on Climate Change* [Masson-Delmotte, V., P. Zhai, A. Pirani, S.L. Connors, C. Péan, S. Berger, N. Caud, Y. Chen, L. Goldfarb, M.I. Gomis, M. Huang, K. Leitzell, E. Lonnoy, J.B.R. Matthews, T.K. Maycock, T. Waterfield, O. Yelekçi, R. Yu, and B. Zhou (Eds.)]. Cambridge University Press. In Press.

Jenerette, G. D., Scott, R. L., & Huxman, T. E. (2008). Whole ecosystem metabolic pulses following precipitation events. *Functional Ecology*, 22(5), 924–930. <https://doi.org/10.1111/j.1365-2435.2008.01450.x>

Jung, M., Reichstein, M., Schwalm, C. R., Huntingford, C., Sitch, S., Ahlström, A., Arneth, A., Camps-Valls, G., Ciais, P., Friedlingstein, P., Gans, F., Ichii, K., Jain, A. K., Kato, E., Papale, D., Poulter, B., Raduly, B., Rödenbeck, C., Tramontana, G., ... Zeng, N. (2017). Compensatory water effects link yearly global land CO<sub>2</sub> sink changes to temperature. *Nature*, 541(7638), 516–520. <https://doi.org/10.1038/nature20780>

Jung, M., Schwalm, C., Migliavacca, M., Walther, S., Camps-Valls, G., Koirala, S., Anthoni, P., Besnard, S., Bodesheim, P., Carvalhais, N., Chevallier, F., Gans, F., Goll, D. S., Haverd, V., Köhler, P., Ichii, K., Jain, A. K., Liu, J., Lombardozzi, D., ... Reichstein, M. (2020). Scaling carbon fluxes from eddy covariance sites to Globe: Synthesis and evaluation of the FLUXCOM approach. *Biogeosciences*, 17(5), 1343–1365. <https://doi.org/10.5194/bg-17-1343-2020>

Kasischke, E. S., Amiro, B. D., Barger, N. N., French, N. H., Goetz, S. J., Grosse, G., Harmon, M. E., Hicke, J. A., Liu, S., & Masek, J. G. (2013). Impacts of disturbance on the terrestrial carbon budget of North America. *Journal of Geophysical Research: Biogeosciences*, 118(1), 303–316. <https://doi.org/10.1002/jgrg.20027>

Keeling, C. D., Chin, J. F., & Whorf, T. P. (1996). Increased activity of northern vegetation inferred from atmospheric CO<sub>2</sub> measurements. *Nature*, 382(6587), 146–149. <https://doi.org/10.1038/382146a0>

Keenan, T. F., Baker, I., Barr, A., Ciais, P., Davis, K., Dietze, M., Dragoni, D., Gough, C. M., Grant, R., Hollinger, D., Hufkens, K., Poulter, B., McCaughey, H., Raczka, B., Ryu, Y., Schaefer, K., Tian, H., Verbeeck, H., Zhao, M., & Richardson, A. D. (2012). Terrestrial biosphere model performance for inter-annual variability of land-atmosphere CO<sub>2</sub> exchange. *Global Change Biology*, 18(6), 1971–1987. <https://doi.org/10.1111/j.1365-2486.2012.02678.x>

Keenan, T. F., Darby, B., Felts, E., Sonnentag, O., Friedl, M. A., Hufkens, K., O’Keefe, J., Klosterman, S., Munger, J. W., Toomey, M., & Richardson, A. D. (2014). Tracking Forest Phenology and seasonal physiology using digital repeat photography: A critical assessment. *Ecological Applications*, 24(6), 1478–1489. <https://doi.org/10.1890/13-0652.1>

Kolby Smith, W., Reed, S. C., Cleveland, C. C., Ballantyne, A. P., Anderson, W. R., Wieder, W. R., Liu, Y. Y., & Running, S. W. (2016).



- Large divergence of satellite and Earth System Model estimates of global terrestrial CO<sub>2</sub> fertilization. *Nature Climate Change*, 6(3), 306–310. <https://doi.org/10.1038/nclimate2879>
- Launiainen, S., Katul, G. G., Leppä, K., Kolari, P., Aslan, T., Grönholm, T., Korhonen, L., Mammarella, I., & Vesala, T. (2022). Does growing atmospheric CO<sub>2</sub> explain increasing carbon sink in a boreal coniferous forest? *Global Change Biology*, 28(9), 2910–2929. <https://doi.org/10.1111/gcb.16117>
- Lenth, R. V. (2022). emmeans: Estimated Marginal Means, aka Least-Squares MeansVersion (R package version 1.7.3.). <https://cran.r-project.org/web/packages/emmeans/>
- Loescher, H. W., Vargas, R., Mirtl, M., Morris, B., Pauw, J., Yu, X., Kutsch, W., Mabee, P., Tang, J., Ruddell, B. L., Pulsifer, P., Bäck, J., Zacharias, S., Grant, M., Feig, G., Zheng, L., Waldmann, C., & Genazzio, M. A. (2022). Building a global ecosystem research infrastructure to address global grand challenges for macrosystem ecology. *Earth's Future*, 10(5). <https://doi.org/10.1029/2020ef001696>
- Lowry, C. S. (2008). *Controls on groundwater flow in a peat dominated wetland/stream complex, allequash wetland, northern Wisconsin* (thesis). University of Wisconsin - Madison, Madison.
- Luo, Y. (2007). Terrestrial carbon-cycle feedback to climate warming. *Annual Review of Ecology, Evolution, and Systematics*, 38(1), 683–712. <https://doi.org/10.1146/annurev.ecolsys.38.091206.095808>
- Luo, Y., Su, B., Currie, W. S., Dukes, J. S., Finzi, A., Hartwig, U., Hungate, B., Mc Murtrie, R. E., Oren, R., Parton, W. J., Pataki, D. E., Shaw, M. R., Zak, D. R., & Field, C. B. (2004). Progressive nitrogen limitation of ecosystem responses to rising atmospheric carbon dioxide. *BioScience*, 54(8), 731–739. [https://doi.org/10.1641/0006-3568\(2004\)054\[0731:pnloer\]2.0.co;2](https://doi.org/10.1641/0006-3568(2004)054[0731:pnloer]2.0.co;2)
- Mackay, D. S., Ahl, D. E., Ewers, B. E., Gower, S. T., Burrows, S. N., Samanta, S., & Davis, K. J. (2002). Effects of aggregated classifications of forest composition on estimates of evapotranspiration in a northern Wisconsin Forest. *Global Change Biology*, 8(12), 1253–1265. <https://doi.org/10.1046/j.1365-2486.2002.00554.x>
- Mackay, D. S., Ewers, B. E., Cook, B. D., & Davis, K. J. (2007). Environmental drivers of evapotranspiration in a shrub wetland and an upland forest in northern Wisconsin. *Water Resources Research*, 43(3). <https://doi.org/10.1029/2006wr005149>
- Marcolla, B., Rödenbeck, C., & Cescatti, A. (2017). Patterns and controls of inter-annual variability in the terrestrial carbon budget. *Biogeosciences*, 14(16), 3815–3829. <https://doi.org/10.5194/bg-14-3815-2017>
- Mathias, J. M., & Thomas, R. B. (2021). Global tree intrinsic water use efficiency is enhanced by increased atmospheric CO<sub>2</sub> and modulated by climate

and plant functional types. *Proceedings of the National Academy of Sciences*, 118(7). <https://doi.org/10.1073/pnas.2014286118>

McDowell, N. G., Allen, C. D., Anderson-Teixeira, K., Aukema, B. H., Bond-Lamberty, B., Chini, L., Clark, J. S., Dietze, M., Grossiord, C., Hanbury-Brown, A., Hurtt, G. C., Jackson, R. B., Johnson, D. J., Kueppers, L., Lichstein, J. W., Ogle, K., Poulter, B., Pugh, T. A., Seidl, R., ... Xu, C. (2020). Pervasive shifts in forest dynamics in a changing world. *Science*, 368(6494). <https://doi.org/10.1126/science.aaz9463>

McDowell, N. G., Sapes, G., Pivovarov, A., Adams, H. D., Allen, C. D., Anderegg, W. R., Arend, M., Breshears, D. D., Brodribb, T., Choat, B., Cochard, H., De Cáceres, M., De Kauwe, M. G., Grossiord, C., Hammond, W. M., Hartmann, H., Hoch, G., Kahmen, A., Klein, T., ... Xu, C. (2022). Mechanisms of woody-plant mortality under rising drought, CO<sub>2</sub> and vapour pressure deficit. *Nature Reviews Earth & Environment*. <https://doi.org/10.1038/s43017-022-00272-1>

Meehl, G. A., Stocker, T. F., Collins, W. D., Friedlingstein, P., Gaye, A. T., Gregory, J. M., Kitoh, A., Knutti, R., Murphy, J. M., Noda, A., Raper, S. C. B., Watterson, I. G., & Weaver, A. J. (2007). Global climate projections. In S. Solomon, D. Qin, M. Manning, Z. Chen, M. Marquis, K. B. Averyt, M. Tignor, & H. L. Miller (Eds.), *Climate change 2007 - The physical science basis. Contribution of Working Group I to the Fourth Assessment Report of the Intergovernmental Panel on Climate Change* (pp. 747–845). Cambridge University Press.

Menzel, A., Sparks, T. H., Estrella, N., Koch, E., Aasa, A., Ahas, R., Alm-Kübler, K., Bissolli, P., Braslavská, O., Briede, A., Chmielewski, F. M., Crepinsek, Z., Curnel, Y., Dahl, Å., Defila, C., Donnelly, A., Filella, Y., Jatczak, K., Måge, F., ... Zust, A. (2006). European phenological response to climate change matches the warming pattern. *Global Change Biology*, 12(10), 1969–1976. <https://doi.org/10.1111/j.1365-2486.2006.01193.x>

Metzger, S. (2018). Surface-atmosphere exchange in a box: Making the control volume a suitable representation for in-situ observations. *Agricultural and Forest Meteorology*, 255, 68–80. <https://doi.org/10.1016/j.agrformet.2017.08.037>

Metzger, S., Junkermann, W., Mauder, M., Butterbach-Bahl, K., Trancón y Widemann, B., Neidl, F., Schäfer, K., Wieneke, S., Zheng, X. H., Schmid, H. P., & Foken, T. (2013). Spatially explicit regionalization of airborne flux measurements using environmental response functions. *Biogeosciences*, 10(4), 2193–2217. <https://doi.org/10.5194/bg-10-2193-2013>

Miao, G., Noormets, A., Domec, J.-C., Trettin, C. C., McNulty, S. G., Sun, G., & King, J. S. (2013). The effect of water table fluctuation on soil respiration in a lower coastal plain forested wetland in the southeastern U.S. *Journal of Geophysical Research: Biogeosciences*, 118(4), 1748–1762. <https://doi.org/10.1002/2013jg002354>

- Migliavacca, M., Musavi, T., Mahecha, M. D., Nelson, J. A., Knauer, J., Baldocchi, D. D., Perez-Priego, O., Christiansen, R., Peters, J., Anderson, K., Bahn, M., Black, T. A., Blanken, P. D., Bonal, D., Buchmann, N., Caldararu, S., Carrara, A., Carvalhais, N., Cescatti, A., ... Reichstein, M. (2021). The three major axes of terrestrial ecosystem function. *Nature*, 598(7881), 468–472. <https://doi.org/10.1038/s41586-021-03939-9>
- Moore, C. E., Meacham-Hensold, K., Lemonnier, P., Slattery, R. A., Benjamin, C., Bernacchi, C. J., Lawson, T., & Cavanagh, A. P. (2021). The effect of increasing temperature on crop photosynthesis: From enzymes to ecosystems. *Journal of Experimental Botany*, 72(8), 2822–2844. <https://doi.org/10.1093/jxb/erab090>
- Morgner, E., Elberling, B., Strebel, D., & Cooper, E. J. (2010). The importance of winter in annual ecosystem respiration in the High Arctic: Effects of snow depth in two vegetation types. *Polar Research*, 29(1), 58–74. <https://doi.org/10.1111/j.1751-8369.2010.00151.x>
- Muggeo, V. M. R. (2008). segmented: an R package to fit regression models with broken-line relationships. *R News*, 8(1), 20–25. <https://cran.r-project.org/doc/Rnews/>
- Murphy, B. A., May, J. A., Butterworth, B. J., Andresen, C. G., & Desai, A. R. (2022). Unravelling forest complexity: Resource use efficiency, disturbance, and the structure-function relationship. *Journal of Geophysical Research: Biogeosciences*, in press, <https://doi.org/10.1029/2021JG006748>
- Niu, B., Zhang, X., Piao, S., Janssens, I. A., Fu, G., He, Y., Zhang, Y., Shi, P., Dai, E., Yu, C., Zhang, J., Yu, G., Xu, M., Wu, J., Zhu, L., Desai, A. R., Chen, J., Bohrer, G., Gough, C. M., ... Ouyang, Z. (2021). Warming homogenizes apparent temperature sensitivity of ecosystem respiration. *Science Advances*, 7(15). <https://doi.org/10.1126/sciadv.abc7358>
- Noda, H. M., Muraoka, H., & Nasahara, K. N. (2021). Plant ecophysiological processes in spectral profiles: Perspective from a deciduous broadleaf forest. *Journal of Plant Research*. <https://doi.org/10.1007/s10265-021-01302-7>
- Novick, K. A., Ficklin, D. L., Stoy, P. C., Williams, C. A., Bohrer, G., Oishi, A. C., Papuga, S. A., Blanken, P. D., Noormets, A., Sulman, B. N., Scott, R. L., Wang, L., & Phillips, R. P. (2016). The increasing importance of atmospheric demand for ecosystem water and carbon fluxes. *Nature Climate Change*, 6(11), 1023–1027. <https://doi.org/10.1038/nclimate3114>
- Novick, K. A., Biederman, J. A., Desai, A. R., Litvak, M. E., Moore, D. J. P., Scott, R. L., & Torn, M. S. (2018). The Ameriflux Network: A coalition of the willing. *Agricultural and Forest Meteorology*, 249, 444–456. <https://doi.org/10.1016/j.agrformet.2017.10.009>
- Novick, K. A., Metzger, S., Anderegg, W. R., Barnes, M., Cala, D. S., Guan, K., Hemes, K. S., Hollinger, D. Y., Kumar, J., Litvak, M., Lombardozi, D., Normile, C. P., Oikawa, P., Runkle, B. R., Torn, M., &

- Wiesner, S. (2022). Informing nature-based climate solutions for the United States with the best-available science. *Global Change Biology*. <https://doi.org/10.1111/gcb.16156>
- Parker, W. C., & Dey, D. C. (2008). Influence of overstory density on ecophysiology of red oak (*Quercus rubra*) and sugar maple (*Acer saccharum*) seedlings in central Ontario Shelterwoods. *Tree Physiology*, 28(5), 797–804. <https://doi.org/10.1093/treephys/28.5.797>
- Pastorello, G., Trotta, C., Canfora, E., Chu, H., Christianson, D., Cheah, Y.-W., Poindexter, C., Chen, J., Elbashandy, A., Humphrey, M., Isaac, P., Polidori, D., Reichstein, M., Ribeca, A., van Ingen, C., Vuichard, N., Zhang, L., Amiro, B., Ammann, C., ... Papale, D. (2020). The FLUXNET2015 dataset and the ONEFlux processing pipeline for Eddy Covariance Data. *Scientific Data*, 7(1). <https://doi.org/10.1038/s41597-020-0534-3>
- Piao, S., Friedlingstein, P., Ciais, P., Viovy, N., & Demarty, J. (2007). Growing season extension and its impact on terrestrial carbon cycle in the Northern Hemisphere over the past 2 decades. *Global Biogeochemical Cycles*, 21(3). <https://doi.org/10.1029/2006gb002888>
- Piao, S., Tan, J., Chen, A., Fu, Y. H., Ciais, P., Liu, Q., Janssens, I. A., Vicca, S., Zeng, Z., Jeong, S.-J., Li, Y., Myneni, R. B., Peng, S., Shen, M., & Peñuelas, J. (2015). Leaf onset in the northern hemisphere triggered by daytime temperature. *Nature Communications*, 6(1). <https://doi.org/10.1038/ncomms7911>
- Piao, S., Liu, Q., Chen, A., Janssens, I. A., Fu, Y., Dai, J., Liu, L., Lian, X., Shen, M., & Zhu, X. (2019a). Plant phenology and global climate change: Current progresses and challenges. *Global Change Biology*, 25(6), 1922–1940. <https://doi.org/10.1111/gcb.14619>
- Piao, S., Zhang, X., Chen, A., Liu, Q., Lian, X., Wang, X., Peng, S., & Wu, X. (2019b). The impacts of climate extremes on the terrestrial carbon cycle: A review. *Science China Earth Sciences*, 62(10), 1551–1563. <https://doi.org/10.1007/s11430-018-9363-5>
- Piao, S., Wang, X., Wang, K., Li, X., Bastos, A., Canadell, J. G., Ciais, P., Friedlingstein, P., & Sitch, S. (2020). Interannual variation of terrestrial carbon cycle: Issues and perspectives. *Global Change Biology*, 26(1), 300–318. <https://doi.org/10.1111/gcb.14884>
- Pinheiro, J., Bates, D., & R Core Team. (2022). nlme: Linear and Nonlinear Mixed Effects Models (R package version 3.1-157). <https://cran.r-project.org/web/packages/nlme/>
- Polgar, C. A., & Primack, R. B. (2011). Leaf-out phenology of temperate woody plants: From trees to ecosystems. *New Phytologist*, 191(4), 926–941. <https://doi.org/10.1111/j.1469-8137.2011.03803.x>
- Polgar, C. A., Gallinat, A., & Primack, R. B. (2014). Drivers of leaf-out phenology and their implications for species invasions: Insights from Thoreau’s Concord. *New Phytologist*, 202(1), 106–115. <https://doi.org/10.1111/nph.12647>

- Post, E., Steinman, B. A., & Mann, M. E. (2018). Acceleration of phenological advance and warming with latitude over the past century. *Scientific Reports*, 8(1), 3927. <https://doi.org/10.1038/s41598-018-22258-0>
- Pugh, C. A., Reed, D. E., Desai, A. R., & Sulman, B. N. (2018). Wetland Flux Controls: How does interacting water table levels and temperature influence carbon dioxide and methane fluxes in Northern Wisconsin? *Biogeochemistry*, 137(1–2), 15–25. <https://doi.org/10.1007/s10533-017-0414-x>.
- Qi, J.-H., Fan, Z.-X., Fu, P.-L., Zhang, Y.-J., & Sterck, F. (2021). Differential determinants of growth rates in subtropical evergreen and deciduous juvenile trees: Carbon gain, hydraulics and nutrient-use efficiencies. *Tree Physiology*, 41(1), 12–23. <https://doi.org/10.1093/treephys/tpaa131>
- R Core Team. (2021). R: A language and environment for statistical computing. R Foundation for Statistical Computing, Vienna, Austria. Retrieved from <https://www.R-project.org/>
- Raupach, M. R., Rayner, P. J., Barrett, D. J., DeFries, R. S., Heimann, M., Ojima, D. S., Quegan, S., & Schimmlus, C. C. (2005). Model-data synthesis in terrestrial carbon observation: Methods, data requirements and data uncertainty specifications. *Global Change Biology*, 11(3), 378–397. <https://doi.org/10.1111/j.1365-2486.2005.00917.x>
- Reichstein, M., Falge, E., Baldocchi, D., Papale, D., Aubinet, M., Berbigier, P., Bernhofer, C., Buchmann, N., Gilmanov, T., Granier, A., Grunwald, T., Havrankova, K., Ilvesniemi, H., Janous, D., Knohl, A., Laurila, T., Lohila, A., Loustau, D., Matteucci, G., ... Valentini, R. (2005). On the separation of net ecosystem exchange into assimilation and ecosystem respiration: Review and improved algorithm. *Global Change Biology*, 11(9), 1424–1439. <https://doi.org/10.1111/j.1365-2486.2005.001002.x>
- Reid, P.C., Hari, R.E., Beaugrand, G., Livingstone, D.M., Marty, C., *et al.* (2016). Global impacts of the 1980s regime shift. *Glob Change Biol*, 22, 682–703. <https://doi.org/10.1111/gcb.13106>
- Restaino, C. M., Peterson, D. L., & Littell, J. (2016). Increased water deficit decreases Douglas fir growth throughout western US forests. *Proceedings of the National Academy of Sciences*, 113(34), 9557–9562. <https://doi.org/10.1073/pnas.1602384113>
- Rhemtulla, J. M., Mladenoff, D. J., & Clayton, M. K. (2009). Legacies of historical land use on regional forest composition and structure in Wisconsin, USA (mid-1800s–1930s–2000s). *Ecological Applications*, 19(4), 1061–1078. <https://doi.org/10.1890/08-1453.1>
- Richardson, A. D., Keenan, T. F., Migliavacca, M., Ryu, Y., Sonnentag, O., & Toomey, M. (2013). Climate change, phenology, and phenological control of vegetation feedbacks to the climate system. *Agricultural and Forest Meteorology*, 169, 156–173. <https://doi.org/10.1016/j.agrformet.2012.09.012>

- Richardson, A. D., Hufkens, K., Milliman, T., Aubrecht, D. M., Chen, M., Gray, J. M., Johnston, M. R., Keenan, T. F., Klosterman, S. T., Kosmala, M., Melaas, E. K., Friedl, M. A., & Froking, S. (2018). Tracking vegetation phenology across diverse North American biomes using PhenoCam imagery. *Scientific Data*, 5(1). <https://doi.org/10.1038/sdata.2018.28>
- Roberts, A. M. I., Tansey, C., Smithers, R. J., & Phillimore, A. B. (2015). Predicting a change in the order of spring phenology in temperate forests. *Global Change Biology*, 21(7), 2603–2611. <https://doi.org/10.1111/gcb.12896>
- Rosell, J. A., Piper, F. I., Jiménez-Vera, C., Vergílio, P. C., Marcati, C. R., Castorena, M., & Olson, M. E. (2020). Inner bark as a crucial tissue for non-structural carbohydrate storage across three tropical Woody Plant Communities. *Plant, Cell & Environment*, 44(1), 156–170. <https://doi.org/10.1111/pce.13903>
- Running, S., Mu, Q., & Zhao, M. (2015). *MOD17A2H MODIS/Terra Gross Primary Productivity 8-Day L4 Global 500m SIN Grid V006* [Data set]. NASA EOSDIS Land Processes DAAC. Accessed 2022-05-06 from <https://doi.org/10.5067/MODIS/MOD17A2H.006>
- Schindlbacher, A., Zechmeister-Boltenstern, S., Kitzler, B., & Jandl, R. (2008). Experimental Forest Soil Warming: Response of autotrophic and heterotrophic soil respiration to a short-term 10°C temperature rise. *Plant and Soil*, 303(1-2), 323–330. <https://doi.org/10.1007/s11104-007-9511-2>
- Schwieger, S., Blume-Werry, G., Peters, B., Smiljanić, M., & Kreyling, J. (2019). Patterns and drivers in spring and autumn phenology differ above- and below-ground in four ecosystems under the same macroclimatic conditions. *Plant and Soil*, 445(1-2), 217–229. <https://doi.org/10.1007/s11104-019-04300-w>
- Scott, R. L., Serrano-Ortiz, P., Domingo, F., Hamerlynck, E. P., & Kowalski, A. S. (2012). Commonalities of carbon dioxide exchange in semiarid regions with monsoon and Mediterranean climates. *Journal of Arid Environments*, 84, 71–79. <https://doi.org/10.1016/j.jaridenv.2012.03.017>
- Seydel, C., Kitashova, A., Fürtauer, L., & Nägele, T. (2022). Temperature-induced dynamics of plant carbohydrate metabolism. *Physiologia Plantarum*, 174(1). <https://doi.org/10.1111/ppl.13602>
- Syednasrollah, B., Young, A. M., Hufkens, K., Milliman, T., Friedl, M. A., Froking, S., Richardson, A. D., Abraha, M., Allen, D. W., Apple, M., Arain, M. A., Baker, J., Baker, J. M., Baldocchi, D., Bernacchi, C. J., Bhattacharjee, J., Blanken, P., Bosch, D. D., Boughton, R., ... Zona, D. (2019). PhenoCam Dataset v2.0: Vegetation Phenology from Digital Camera Imagery, 2000-2018 (Version 2). ORNL Distributed Active Archive Center. <https://doi.org/10.3334/ORNLDAAAC/1674>
- Sikma, M., Vilà-Guerau de Arellano, J., Pedruzo-Bagazgoitia, X., Voskamp, T., Heusinkveld, B. G., Anten, N. P. R., & Evers, J. B. (2019). Impact

of future warming and enhanced [CO<sub>2</sub>] on the vegetation-cloud interaction. *Journal of Geophysical Research: Atmospheres*, 124(23), 12444–12454. <https://doi.org/10.1029/2019jd030717>

Soil Survey Staff (2022). *Natural Resources Conservation Service, United States Department of Agriculture. Soil Survey Geographic (SSURGO) Database*. Available online at <https://sdmdataaccess.sc.egov.usda.gov>. Accessed April 26, 2022.

Sperry, J. S., Venturas, M. D., Todd, H. N., Trugman, A. T., Anderegg, W. R., Wang, Y., & Tai, X. (2019). The impact of Rising CO<sub>2</sub> and acclimation on the response of us forests to global warming. *Proceedings of the National Academy of Sciences*, 116(51), 25734–25744. <https://doi.org/10.1073/pnas.1913072116>

Stettz, S. G., Parazoo, N. C., Bloom, A. A., Blanken, P. D., Bowling, D. R., Burns, S. P., Bacour, C., Maignan, F., Raczka, B., Norton, A. J., Baker, I., Williams, M., Shi, M., Zhang, Y., & Qiu, B. (2022). Resolving temperature limitation on spring productivity in an evergreen conifer forest using a model–data fusion framework. *Biogeosciences*, 19(2), 541–558. <https://doi.org/10.5194/bg-19-541-2022>

Stoy, P. C., Richardson, A. D., Baldocchi, D. D., Katul, G. G., Stanovick, J., Mahecha, M. D., Reichstein, M., Detto, M., Law, B. E., Wohlfahrt, G., Arriga, N., Campos, J., McCaughey, J. H., Montagnani, L., Paw U, K. T., Sevanto, S., & Williams, M. (2009). Biosphere-atmosphere exchange of CO<sub>2</sub> in relation to climate: A cross-biome analysis across multiple time scales. *Biogeosciences*, 6(10), 2297–2312. <https://doi.org/10.5194/bg-6-2297-2009>

Strack, M., & Waddington, J. M. (2007). Response of peatland carbon dioxide and methane fluxes to a water table drawdown experiment. *Global Biogeochemical Cycles*, 21(1). <https://doi.org/10.1029/2006gb002715>

Sulman, B. N., Desai, A. R., Cook, B. D., Saliendra, N., & Mackay, D. S. (2009). Contrasting carbon dioxide fluxes between a drying shrub wetland in northern Wisconsin, USA, and nearby forests. *Biogeosciences*, 6(6), 1115–1126. <https://doi.org/10.5194/bg-6-1115-2009>

Sulman, B. N., Desai, A. R., Saliendra, N. Z., Lafleur, P. M., Flanagan, L. B., Sonnentag, O., Mackay, D. S., Barr, A. G., & van der Kamp, G. (2010). CO<sub>2</sub> fluxes at northern fens and bogs have opposite responses to inter-annual fluctuations in water table. *Geophysical Research Letters*, 37(19). <https://doi.org/10.1029/2010gl044018>

Sutinen, S., Partanen, J., Vihera-Aarnio, A., & Hakkinen, R. (2009). Anatomy and morphology in developing vegetative buds on detached Norway spruce branches in controlled conditions before Bud Burst. *Tree Physiology*, 29(11), 1457–1465. <https://doi.org/10.1093/treephys/tpp078>

Tang, J., Bolstad, P. V., Ewers, B. E., Desai, A. R., Davis, K. J., & Carey, E. V. (2006). Sap flux-upscaled canopy transpiration, stomatal conductance, and water use efficiency in an old growth forest in the Great Lakes region of

- the United States. *Journal of Geophysical Research: Biogeosciences*, 111(G2). <https://doi.org/10.1029/2005jg000083>
- Tang, J., Bolstad, P. V., Desai, A. R., Martin, J. G., Cook, B. D., Davis, K. J., & Carey, E. V. (2008). Ecosystem respiration and its components in an old-growth forest in the Great Lakes region of the United States. *Agricultural and Forest Meteorology*, 148(2), 171–185. <https://doi.org/10.1016/j.agrformet.2007.08.008>
- Tang, X., Shi, Y., Luo, X., Liu, L., Jian, J., Bond-Lamberty, B., Hao, D., Olchev, A., Zhang, W., Gao, S., & Li, J. (2021). A decreasing carbon allocation to below-ground autotrophic respiration in global forest ecosystems. *Science of The Total Environment*, 798, 149273. <https://doi.org/10.1016/j.scitotenv.2021.149273>
- Terrer, C., Jackson, R. B., Prentice, I. C., Keenan, T. F., Kaiser, C., Vicca, S., Fisher, J. B., Reich, P. B., Stocker, B. D., Hungate, B. A., Peñuelas, J., McCal-lum, I., Soudzilovskaia, N. A., Cernusak, L. A., Talhelm, A. F., Van Sundert, K., Piao, S., Newton, P. C., Hovenden, M. J., ... Franklin, O. (2019). Nitrogen and phosphorus constrain the CO<sub>2</sub> fertilization of global plant biomass. *Nature Climate Change*, 9(9), 684–689. <https://doi.org/10.1038/s41558-019-0545-2>
- Thompson R. & Clark R. M. (2008). Is spring starting earlier? *The Holocene*, 18(1), 95-104. <https://doi.org/10.1177/0959683607085599>
- Tixier, A., Gambetta, G. A., Godfrey, J., Orozco, J., & Zwieniecki, M. A. (2019). Non-structural carbohydrates in dormant woody perennials; The tale of winter survival and spring arrival. *Frontiers in Forests and Global Change*, 2. <https://doi.org/10.3389/ffgc.2019.00018>
- Turner, J., Desai, A. R., Thom, J., Wickland, K. P., & Olson, B. (2019). Wind sheltering impacts on land-atmosphere fluxes over fens. *Frontiers in Environmental Science*, 7. <https://doi.org/10.3389/fenvs.2019.00179>
- Turner, J., Desai, A. R., Thom, J., & Wickland, K. P. (2021). Lagged wetland CH<sub>4</sub> flux response in a historically wet year. *Journal of Geophysical Research: Biogeosciences*, 126(11). <https://doi.org/10.1029/2021jg006458>
- Vargas, R., Sánchez-Cañete P., E., Serrano-Ortiz, P., Curiel Yuste, J., Domingo, F., López-Ballesteros, A., & Oyonarte, C. (2018). Hot-moments of soil CO<sub>2</sub> efflux in a water-limited grassland. *Soil Systems*, 2(3), 47. <https://doi.org/10.3390/soilsystems2030047>
- Walker, B. J., VanLoocke, A., Bernacchi, C. J., & Ort, D. R. (2016). The costs of photorespiration to food production now and in the future. *Annual Review of Plant Biology*, 67(1), 107–129. <https://doi.org/10.1146/annurev-arplant-043015-111709>
- Walther, G.-R., Post, E., Convey, P., Menzel, A., Parmesan, C., Beebee, T. J., Fromentin, J.-M., Hoegh-Guldberg, O., & Bairlein, F. (2002). Ecological responses to recent climate change. *Nature*, 416(6879), 389–395. <https://doi.org/10.1038/416389a>
- Wang, J., Liu, D., Ciais, P., & Peñuelas, J. (2022). Decreasing rainfall frequency



contributes to earlier leaf onset in northern ecosystems. *Nature Climate Change*, 12(4), 386–392. <https://doi.org/10.1038/s41558-022-01285-w>

Wang, M., Sun, R., Zhu, A., & Xiao, Z. (2020). Evaluation and comparison of light use efficiency and gross primary productivity using three different approaches. *Remote Sensing*, 12(6), 1003. <https://doi.org/10.3390/rs12061003>

Wang, T., Ciais, P., Piao, S. L., Ottlé, C., Brender, P., Maignan, F., Arain, A., Cescatti, A., Gianelle, D., Gough, C., Gu, L., Lafleur, P., Laurila, T., Marcolla, B., Margolis, H., Montagnani, L., Moors, E., Saigusa, N., Vesala, T., ... Verma, S. (2011). Controls on winter ecosystem respiration in temperate and boreal ecosystems. *Biogeosciences*, 8(7), 2009–2025. <https://doi.org/10.5194/bg-8-2009-2011>

Wang, W., Davis, K. J., Cook, B. D., Butler, M. P., & Ricciuto, D. M. (2006). Decomposing co2fluxes measured over a mixed ecosystem at a tall tower and extending to a region: A case study. *Journal of Geophysical Research: Biogeosciences*, 111(G2). <https://doi.org/10.1029/2005jg000093>

Wang, X., Liu, L., Piao, S., Janssens, I. A., Tang, J., Liu, W., Chi, Y., Wang, J., & Xu, S. (2014). Soil respiration under climate warming: Differential response of heterotrophic and autotrophic respiration. *Global Change Biology*, 20(10), 3229–3237. <https://doi.org/10.1111/gcb.12620>

Wilder, L., & Boyd, J. N. (2016). Ecophysiological responses of *Tsuga canadensis* (Eastern Hemlock) to projected atmospheric CO<sub>2</sub> and warming. *Southeastern Naturalist*, 15(4), 697–713. <https://doi.org/10.1656/058.015.0412>

Winderlich, J., Gerbig, C., Kolle, O., & Heimann, M. (2014). Inferences from CO<sub>2</sub> and CH<sub>4</sub> concentration profiles at the Zotino Tall Tower Observatory (ZOTTO) on regional summertime ecosystem fluxes. *Biogeosciences*, 11(7), 2055–2068. <https://doi.org/10.5194/bg-11-2055-2014>

Wisconsin Department of Natural Resources. (2016). WISCLAND 2 Land Cover (Level 4), Wisconsin 2016. GeoData@Wisconsin. Retrieved December 20, 2021, from <https://geodata.wisc.edu/catalog/F283F43D-D95E-4CC9-ACBF-859C1A5DEC60>

Wu, C., Wang, X., Wang, H., Ciais, P., Peñuelas, J., Myneni, R. B., Desai, A. R., Gough, C. M., Gonsamo, A., Black, A. T., Jassal, R. S., Ju, W., Yuan, W., Fu, Y., Shen, M., Li, S., Liu, R., Chen, J. M., & Ge, Q. (2018). Contrasting responses of autumn-leaf senescence to daytime and night-time warming. *Nature Climate Change*, 8(12), 1092–1096. <https://doi.org/10.1038/s41558-018-0346-z>

Wutzler, T., Lucas-Moffat, A., Migliavacca, M., Knauer, J., Sickel, K., Šigut, L., Menzer, O., & Reichstein, M. (2018). Basic and extensible post-processing of eddy covariance flux data with reddyproc. *Biogeosciences*, 15(16), 5015–5030. <https://doi.org/10.5194/bg-15-5015-2018>

Xiao, J., Davis, K. J., Urban, N. M., Keller, K., & Saliendra, N. Z. (2011). Upscaling carbon fluxes from towers to the regional scale: Influence of parameter

variability and land cover representation on regional flux estimates. *Journal of Geophysical Research*, 116(G3). <https://doi.org/10.1029/2010jg001568>

Xiao, J., Ollinger, S. V., Frohking, S., Hurtt, G. C., Hollinger, D. Y., Davis, K. J., Pan, Y., Zhang, X., Deng, F., Chen, J., Baldocchi, D. D., Law, B. E., Arain, M. A., Desai, A. R., Richardson, A. D., Sun, G., Amiro, B., Margolis, H., Gu, L., ... Suyker, A. E. (2014). Data-driven diagnostics of terrestrial carbon dynamics over North America. *Agricultural and Forest Meteorology*, 197, 142–157. <https://doi.org/10.1016/j.agrformet.2014.06.013>

Xiao, X., Zhang, Q., Braswell, B., Urbanski, S., Boles, S., Wofsy, S., Moore III, B., and Ojima, D. (2004). Modeling gross primary production of temperate deciduous broadleaf forest using satellite images and climate data. *Remote sensing of environment* 91, no. 2: 256–270. <https://doi.org/10.1016/j.rse.2004.03.010>

Xu, H., Xiao, J., Zhang, Z., Ollinger, S. V., Hollinger, D. Y., Pan, Y., & Wan, J. (2020a). Canopy photosynthetic capacity drives contrasting age dynamics of resource use efficiencies between mature temperate evergreen and deciduous forests. *Global Change Biology*, 26(11), 6156–6167. <https://doi.org/10.1111/gcb.15312>

Xu, K., Metzger, S., & Desai, A. R. (2017). Upscaling tower-observed turbulent exchange at fine spatio-temporal resolution using environmental response functions. *Agricultural and Forest Meteorology*, 232, 10–22. <https://doi.org/10.1016/j.agrformet.2016.07.019>

Xu, K., Sühling, M., Metzger, S., Durden, D., & Desai, A. R. (2020b). Can data mining help eddy covariance see the landscape? A large-eddy simulation study. *Boundary-Layer Meteorology*, 176(1), 85–103. <https://doi.org/10.1007/s10546-020-00513-0>

Yan, T., Song, H., Wang, Z., Teramoto, M., Wang, J., Liang, N., Ma, C., Sun, Z., Xi, Y., Li, L., & Peng, S. (2019). Temperature sensitivity of soil respiration across multiple time scales in a temperate plantation forest. *Science of The Total Environment*, 688, 479–485. <https://doi.org/10.1016/j.scitotenv.2019.06.318>

Yu, Z., Griffis, T. J., & Baker, J. M. (2021). Warming temperatures lead to reduced summer carbon sequestration in the U.S. corn belt. *Communications Earth & Environment*, 2(1). <https://doi.org/10.1038/s43247-021-00123-9>

Yun, J., Jeong, S. J., Ho, C. H., Park, C. E., Park, H., & Kim, J. (2018). Influence of winter precipitation on spring phenology in boreal forests. *Global Change Biology*, 24(11), 5176–5187. <https://doi.org/10.1111/gcb.14414>

Yuste, J. C., Janssens, I. A., Carrara, A., Meiresonne, L., & Ceulemans, R. (2003). Interactive effects of temperature and precipitation on soil respiration in a temperate maritime pine forest. *Tree Physiology*, 23(18), 1263–1270. <https://doi.org/10.1093/treephys/23.18.1263>

Zscheischler, J., Fatichi, S., Wolf, S., Blanken, P., Bohrer, G., Clark, K., Desai, A.R., Hollinger, D., Keenan, T., Novick, K.A., and Seneviratne, S.I. (2016).

Short-term favorable weather conditions are an important control of interannual variability in carbon and water fluxes. *J. Geophys. Res. - G.*, 121, <https://doi.org/10.1002/2016JG003503>.

Zhang, P., Chen, S., Zhang, W., Miao, H., Chen, J., Han, X., & Lin, G. (2012). Biophysical regulations of NEE light response in a steppe and a cropland in inner Mongolia. *Journal of Plant Ecology*, 5(2), 238–248. <https://doi.org/10.1093/jpe/rtr017>

Zhang, X.-Y., Niu, G.-Y., & Zeng, X. (2022). The control of plant and soil hydraulics on the interannual variability of plant carbon uptake over the central US. *Journal of Geophysical Research: Atmospheres*, 127, e2021JD035969. <https://doi.org/10.1029/2021JD035969>

Zhang, Z., Zhao, L., & Lin, A. (2020). Evaluating the performance of Sentinel-3A OLCI Land Products for gross primary productivity estimation using Ameriflux Data. *Remote Sensing*, 12(12), 1927. <https://doi.org/10.3390/rs12121927>

Zhou, Y. (2020). Relative contribution of growing season length and amplitude to long-term trend and interannual variability of vegetation productivity over Northeast China. *Forests*, 11(1), 112. <https://doi.org/10.3390/f11010112>

Zhu, P., Kim, T., Jin, Z., Lin, C., Wang, X., Ciais, P., Mueller, N. D., Aghakouchak, A., Huang, J., Mulla, D., & Makowski, D. (2022). The critical benefits of snowpack insulation and snowmelt for winter wheat productivity. *Nature Climate Change*, 12(5), 485–490. <https://doi.org/10.1038/s41558-022-01327-3>

## Tables

**Table 1.** Description of the the long-term flux tower sites.

<b>Site ID</b>	US-PFa	US-WCr
<b>Name</b>	Park Falls WLEF	Willow Creek
<b>Latitude</b>	45.9459	45.8059
<b>Longitude</b>	-90.2723	-90.0799
<b>Description</b>	Regional tall tower	Mature marsh
<b>PFT</b>	MF	DBF
<b>Years (full years)</b>	1997-present	1999-2006, 2010-present
<b>Ameriflux DOI</b>	10.17190/AMF/1246090	10.17190/AMF/1246090
<b>Key publications</b>	Berger <i>et al.</i> , 2001; Davis <i>et al.</i> , 2003; Desai, 2014; Desai, Xu <i>et al.</i> , 2015	Cook <i>et al.</i> , 2005; Desai, 2014; Desai, Xu <i>et al.</i> , 2015

**Table 2.** Average, maximum, and minimum climate variables from data sources shown in Figure 1.

Variable	Units	Mean	Min	Max
Air temperature	degrees C	5.24	2.99	7.54
Precipitation	mm	852	585	1146

Snowfall	cm	226	98.8	378
VPD	Pa	328	221	433
CO <sub>2</sub>	ppm	392.6	368.5	418.7
Incoming Shortwave	W m <sup>-2</sup>	153	133	167
Start of Season (US-WCr)	day of year	132.33	126	141
Peak G <sub>cc</sub> (US-WCr)	day of year	152.56	141	163
End of Season (US-WCr)	day of year	272.11	264	278

**Table 3.** Annual and seasonal (GS = growing season, NGS = non-growing season) drivers on average annual net ecosystem exchange of CO<sub>2</sub> (NEE), Gross primary productivity (GPP), ecosystem respiration (R<sub>eco</sub>), maximum photosynthetic capacity (A<sub>max</sub>), dark respiration (R<sub>d</sub>), quantum yield ( ), R<sub>10</sub> and temperature sensitivity (Q<sub>10</sub>), where plus signs indicate an increase, and negative sign a decrease, the star (\*) indicates a significant difference among levels and empty cells indicate no change. Green colors denote significant trends at the 95% level.

	NEE	GPP	R <sub>eco</sub>	A <sub>max</sub>	R <sub>d</sub>	R <sub>10</sub>	Q <sub>10</sub>
VPD							+
VPD <sub>GS</sub>		+					
VPD <sub>NGS</sub>			+				
T <sub>air</sub>			+				
T <sub>airGS</sub>			-	+	+		
T <sub>airNGS</sub>	+					-	
TA <sub>GS</sub>	+						
TA <sub>NGS</sub>							
Rain <sub>GS</sub>							
Rain <sub>NGS</sub>	+					+	+
Snow <sub>NGS</sub>					+		
GS <sub>length</sub>				+	+	+	
CO <sub>2</sub>				+	+	+	
Site	*	*	*	*	*	*	*

**Table 4.** Mean annual total NEE, GPP, R<sub>eco</sub> for the long-term sites.

Fluxes		Region	Forests		Wetlands	
		US-PFa	US-WCr	US-Syv	US-Los	US-ALQ
NEE gC m <sup>-2</sup> yr <sup>-1</sup>	Mean	-3.7	-253	-118	-91	-84
	Min	-170	-478	-271	-162	-124
	Max	163	62.7	109	-9.2	-41
GPP gC m <sup>-2</sup> yr <sup>-1</sup>	Mean	878	1174	1339	909	1077
	Min	550	962	1012	712	990
	Max	1098	1552	1619	1070	1223

$R_{eco}$ gC m <sup>-2</sup> yr <sup>-1</sup>	<b>Mean</b>	874	920	1220	818	992
	<b>Min</b>	449	705	818	657	893
	<b>Max</b>	1191	1154	1473	1058	1181
<b>Years</b>	<b>n</b>	24	18	13	16	3

**Table 5.** Major disturbance or climatic events that may have impacted the carbon cycle across the region

<b>Year</b>	<b>Event</b>
1998	ENSO+, warm/dry summer
2001	Forest tent caterpillar defoliation at US-WCr, June
2002-2008	Water table decline at US-Los
2010	Water table rises at US-Los
2012	Early, warm spring, summer Midwest drought
2013	Winter thinning harvest 15% biomass US-WCr
2014	Winter thinning harvest 15% biomass US-WCr
2016	ENSO+
2017	Overstory live tree mortality US-Syv, May
2018	Overstory dead tree mortality US-Syv, Nov

## Figures

**Figure 1.** Map of long-term and CHEESEHEAD19 eddy covariance flux towers. Shapes represent land cover type. Colors indicate seasonal NEE [gC m<sup>-2</sup>] for the period June 20<sup>th</sup> - September 30<sup>th</sup>, 2019.

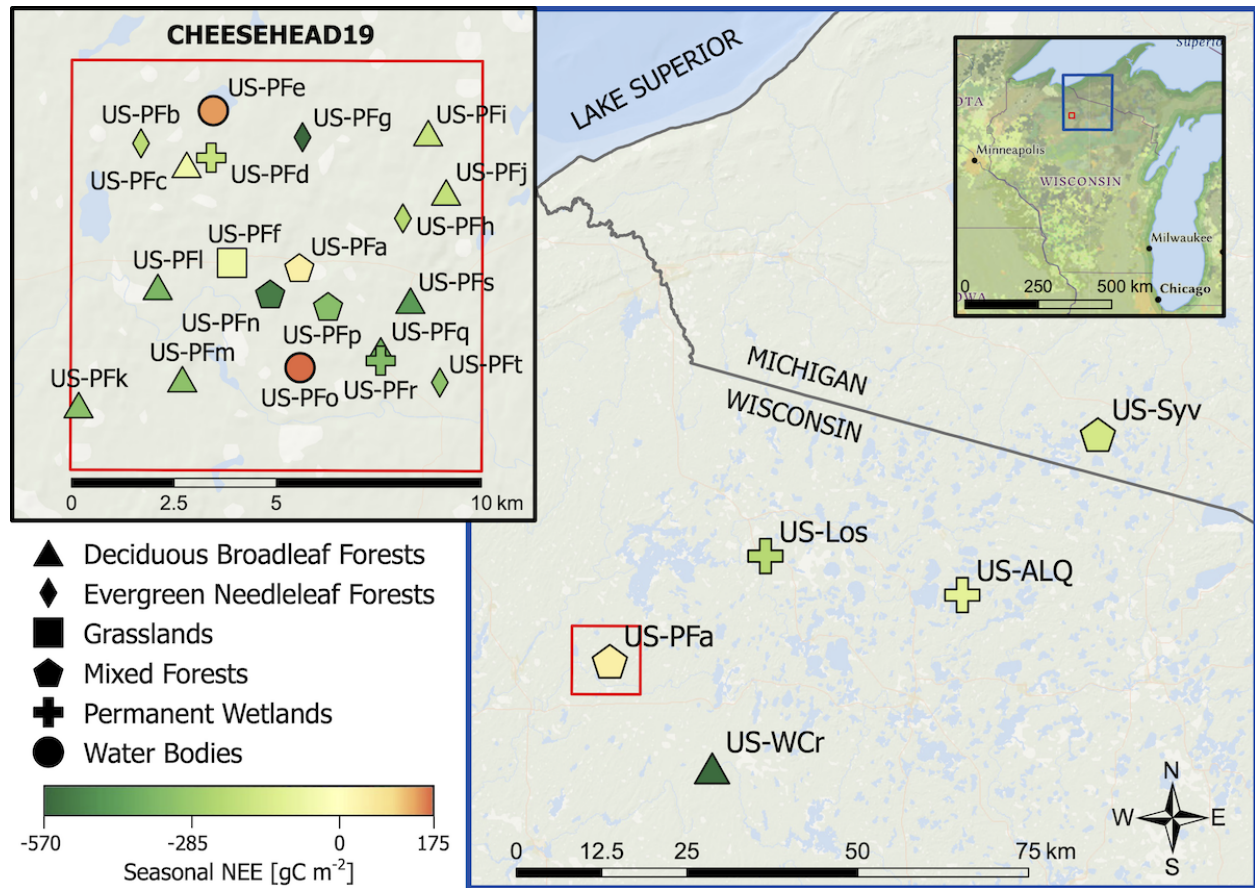


**Figure 2.** Average a) annual and growing season (Jun-Sept) air temperature (red, right axis), b) annual total precipitation and snowfall (blue, right axis), c) annual average incoming shortwave radiation, d) annual average vapor pressure deficit, and e) annual average CO<sub>2</sub> mole fraction based on hourly gap-filled measurements made at the US-PFa very tall tower at 30 m (air temperature, vapor pressure deficit, CO<sub>2</sub>) or surface (shortwave radiation), or Minocqua Dam site (precipitation, snowfall) from 1997-2020.

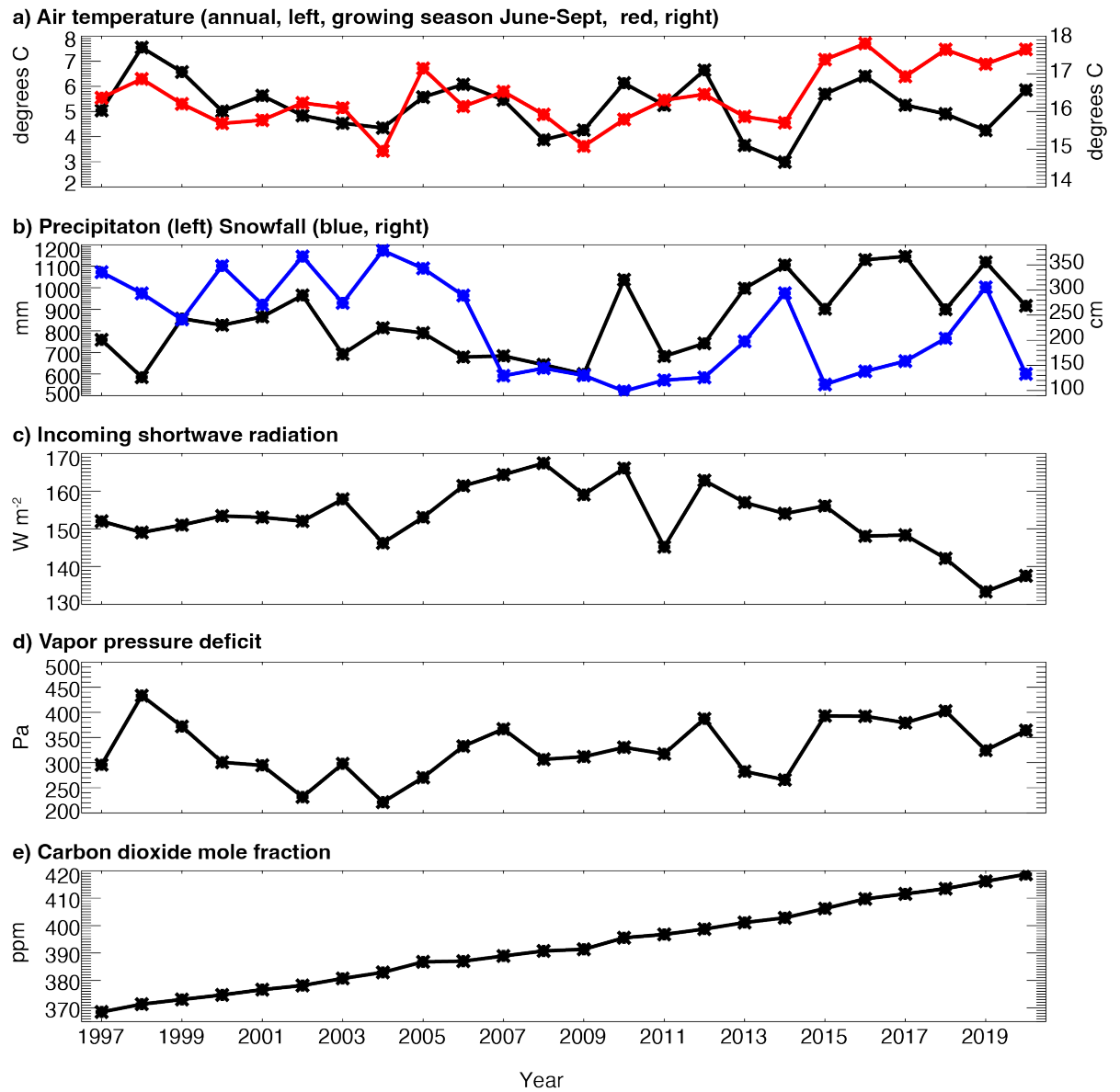


**Figure 3.** PhenoCam derived day of year (DOY) for leaf on (green), maximum green chromatic coordinate (GCC), leaf off (yellow) for a) US-Los, b) US-WCr, c) US-Syv (deciduous component)

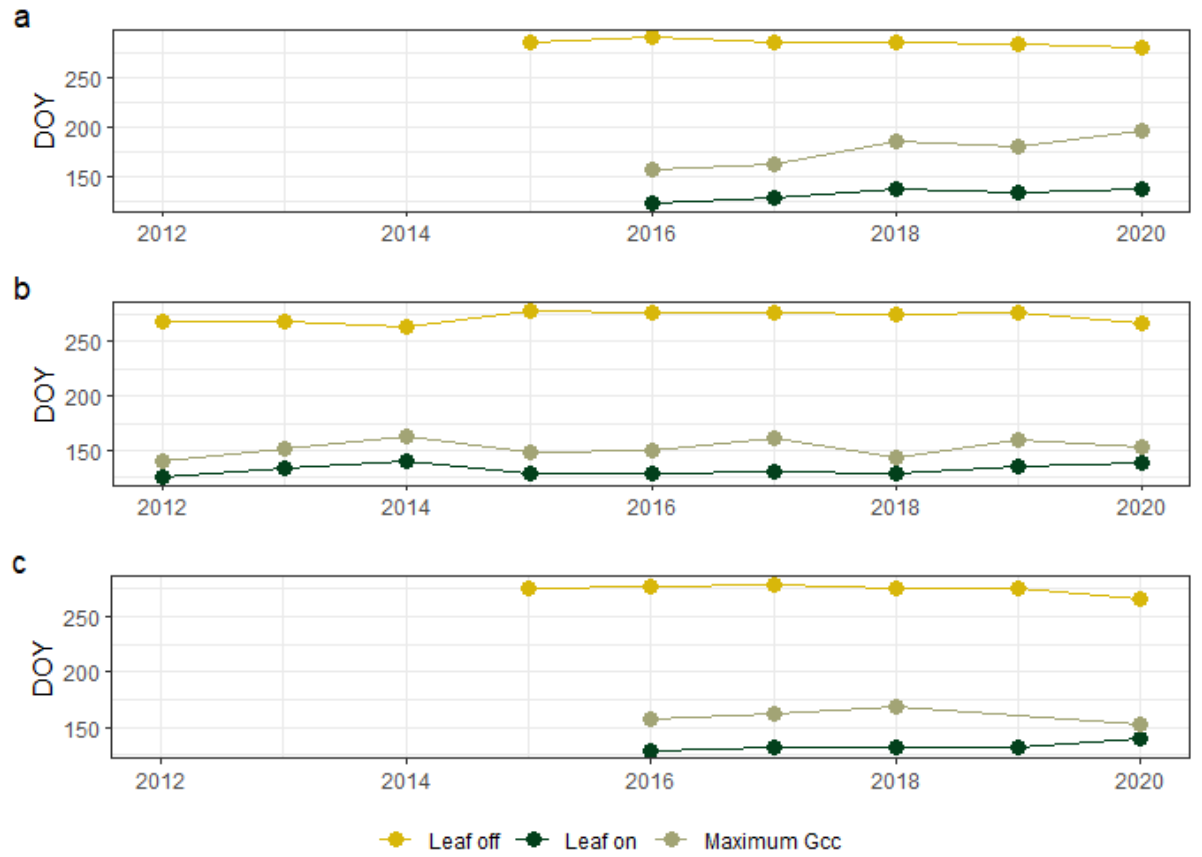


**Figure 4.** Annual gap-filled total a) net ecosystem exchange and partitioned b) gross primary productivity and c) ecosystem respiration for the regional (US-PFa, black), forests (US-WCr and US-Syv) and wetlands (US-Los, US-ALQ) from 1997-2020. Estimated uncertainty shown in shading for each.



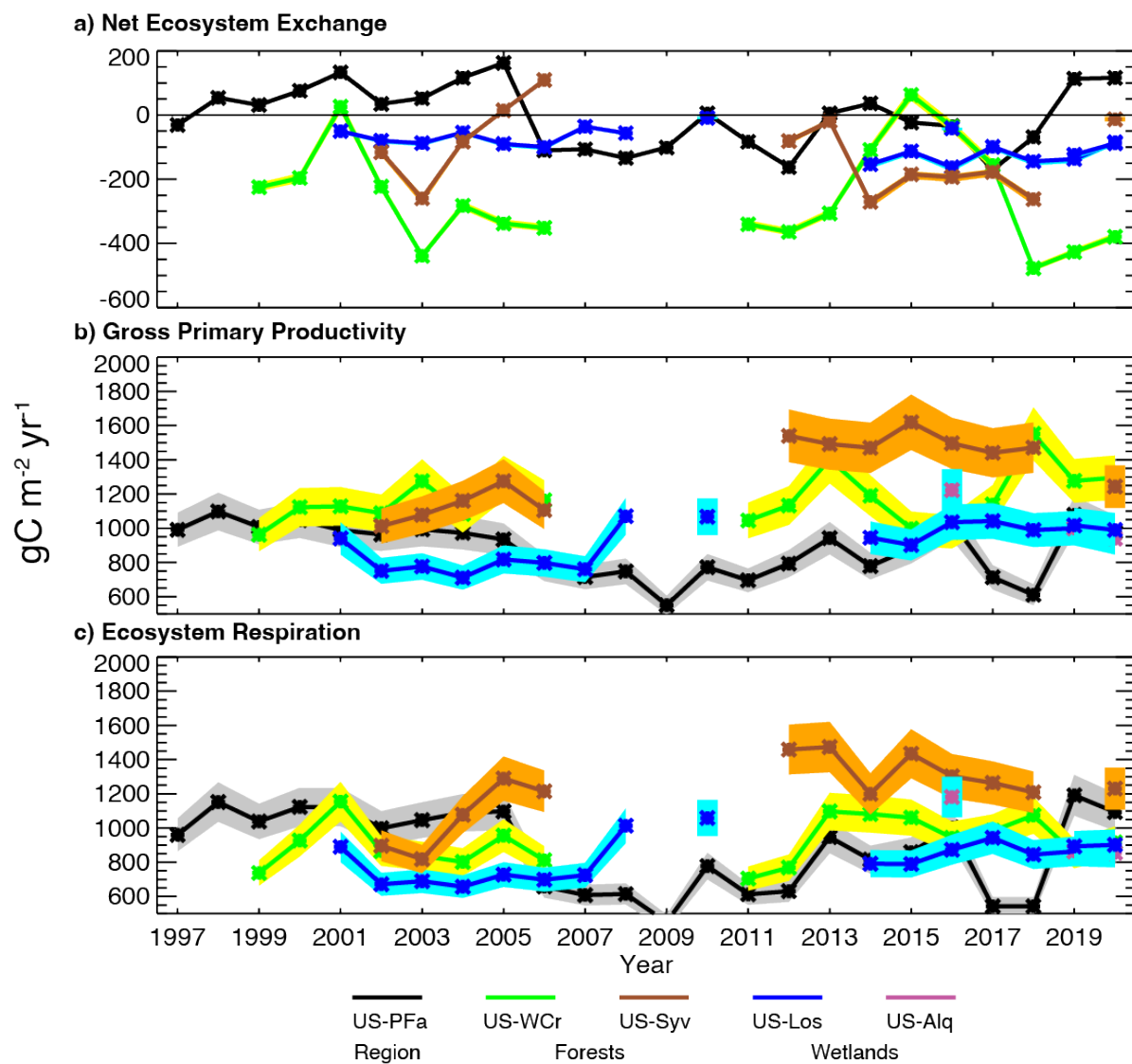


**Figure 5.** Five-day smoothed ensemble daily average NEE, GPP, and  $R_{eco}$  for the five long-term study sites across all years of record. Shading represents 25th and 75th percentile interannual variation (not included for US-ALQ, since < 4 years of data)

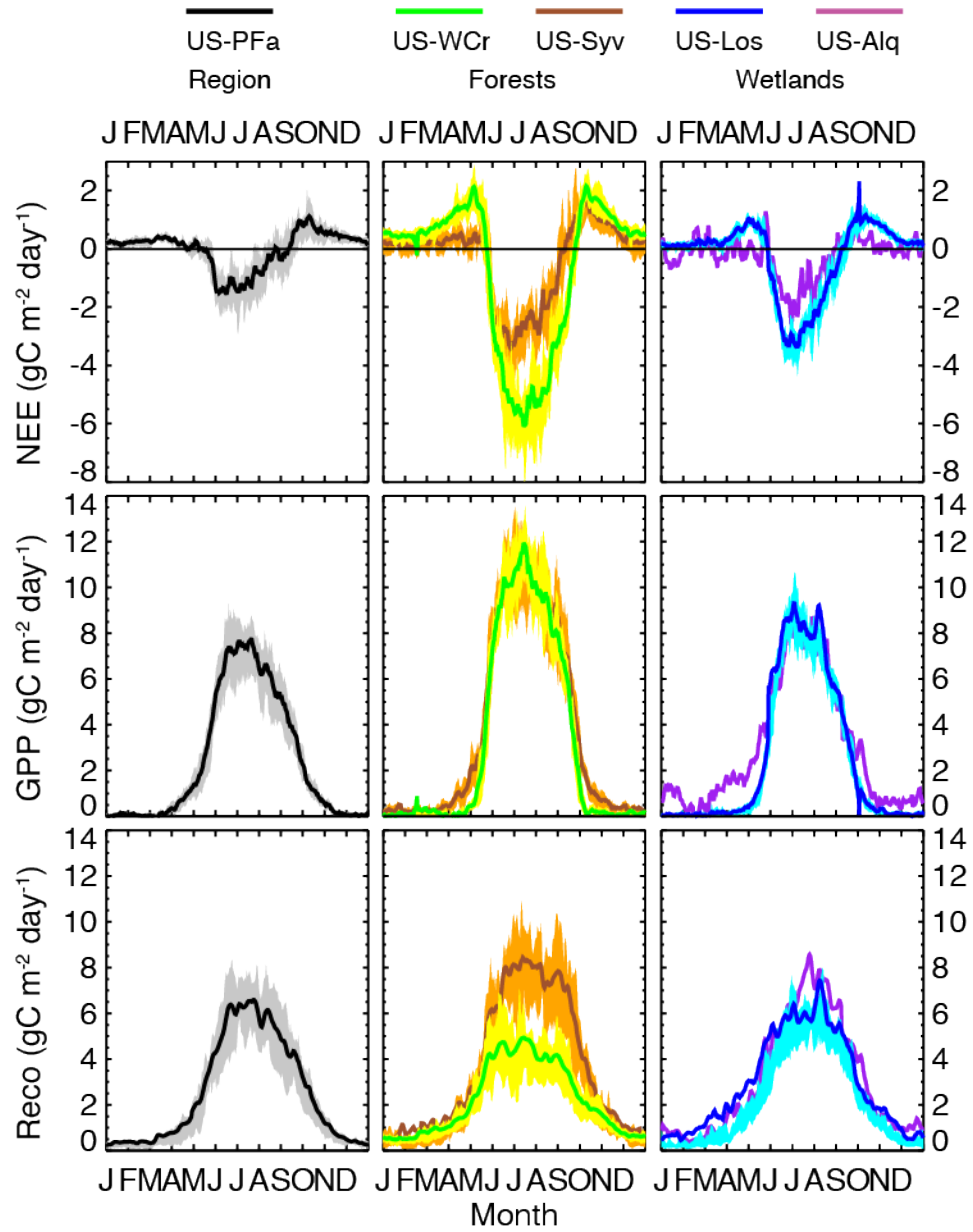


**Figure 6.** Ensemble June-August hourly average NEE, GPP, and  $R_{\text{eco}}$  for the five long-term study sites across all years of record. Shading represents 25th and 75th percentile interannual variation

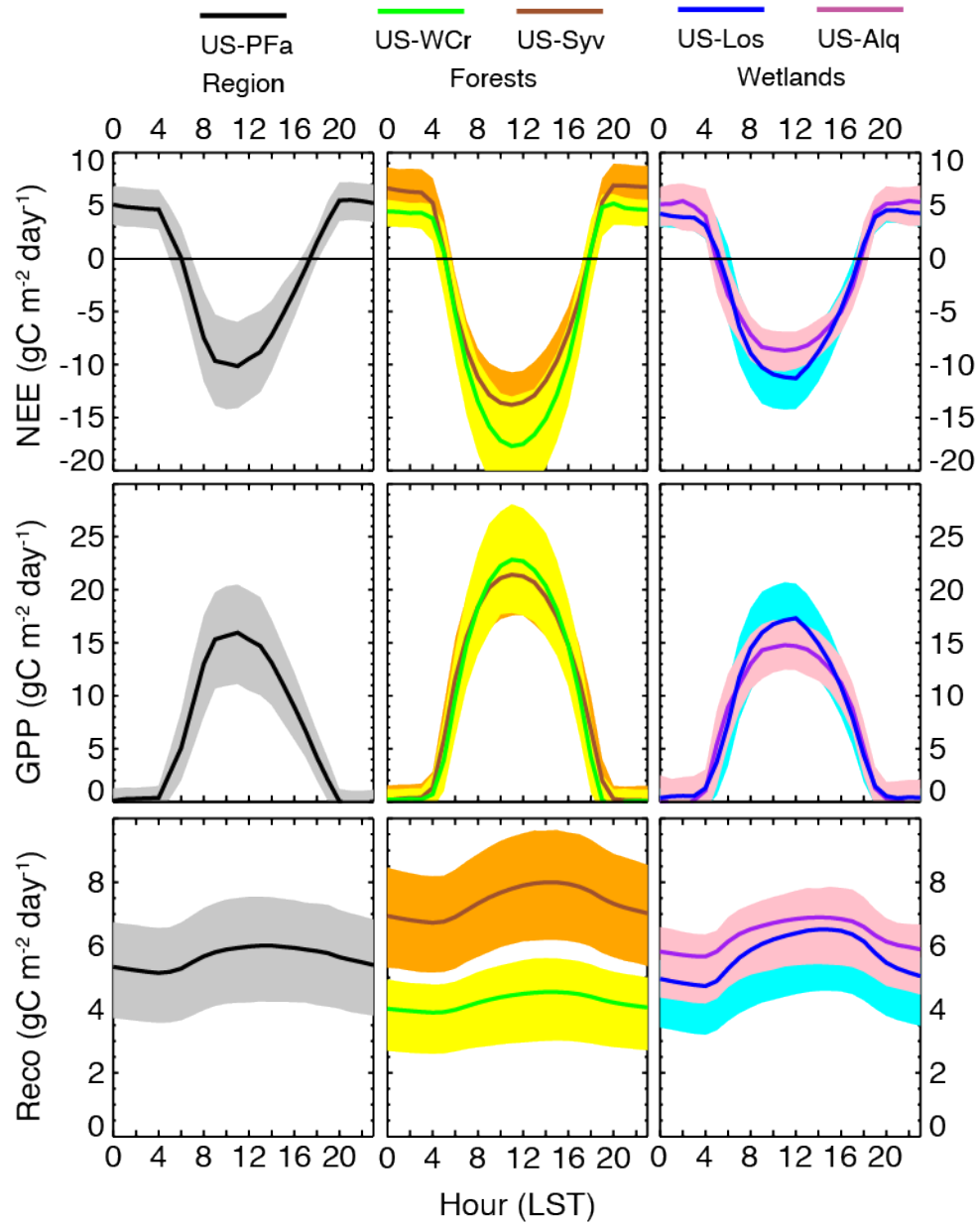


**Figure 7.** Comparison of 2019 June-Sept mean daily NEE (top), GPP (middle), and  $R_{eco}$  (bottom) from CHEESEHEAD19 towers (circles) and the long-term flux towers (squares) for the region, forests and fields, and wetlands and lakes (GPP and  $R_{eco}$  not calculated for lakes). Bars bracket maximum to minimum range of June-Sept NEE observed in other years for the long-term sites

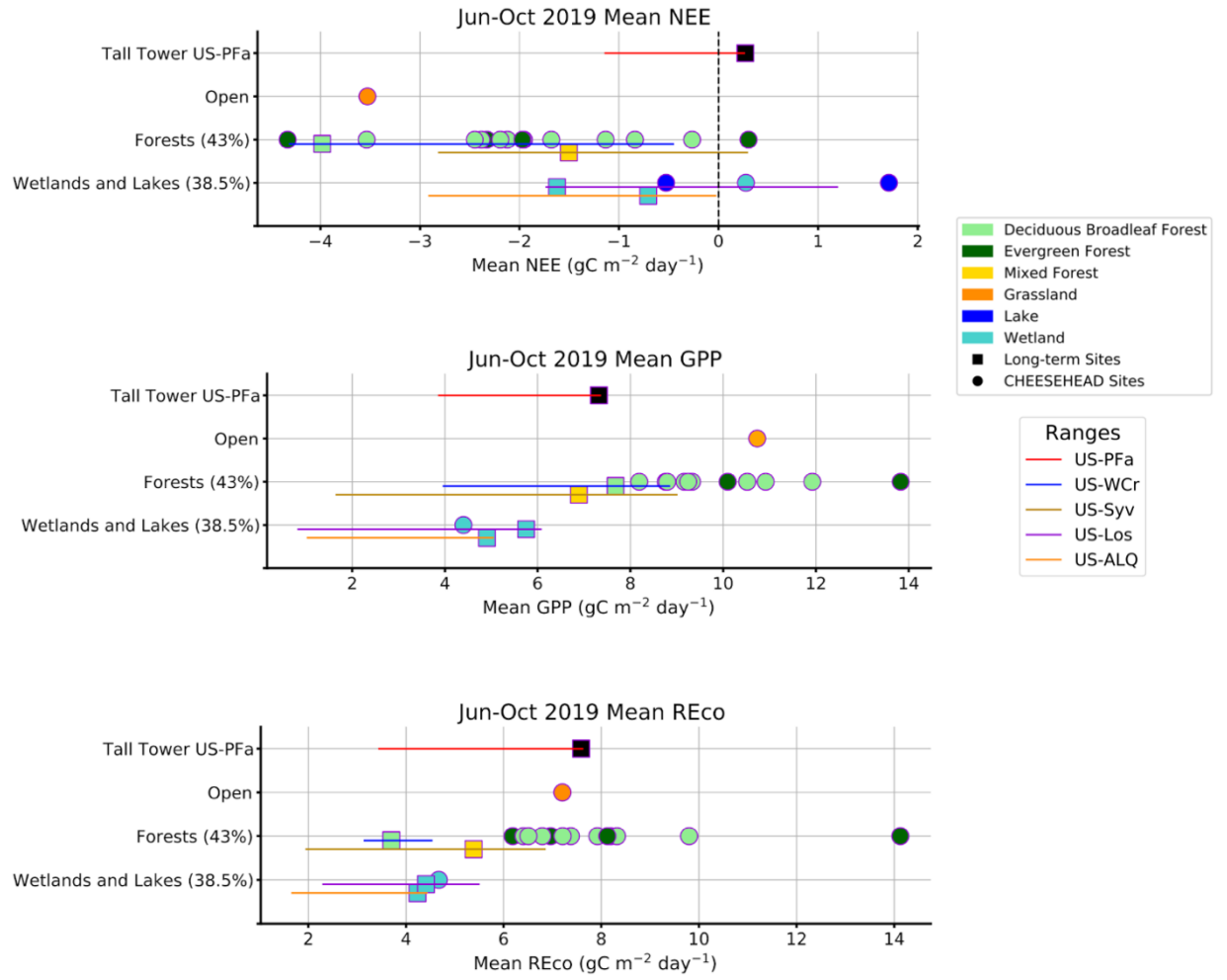


**Figure 8.** Relationship of a) the photosynthetic maximum assimilation parameter ( $A_{\text{max}}$ ) and b) the respiration temperature sensitivity parameter ( $Q_{10}$ ) to VPD (x-axis) and temperature (color) for the five tower sites, including best fit.

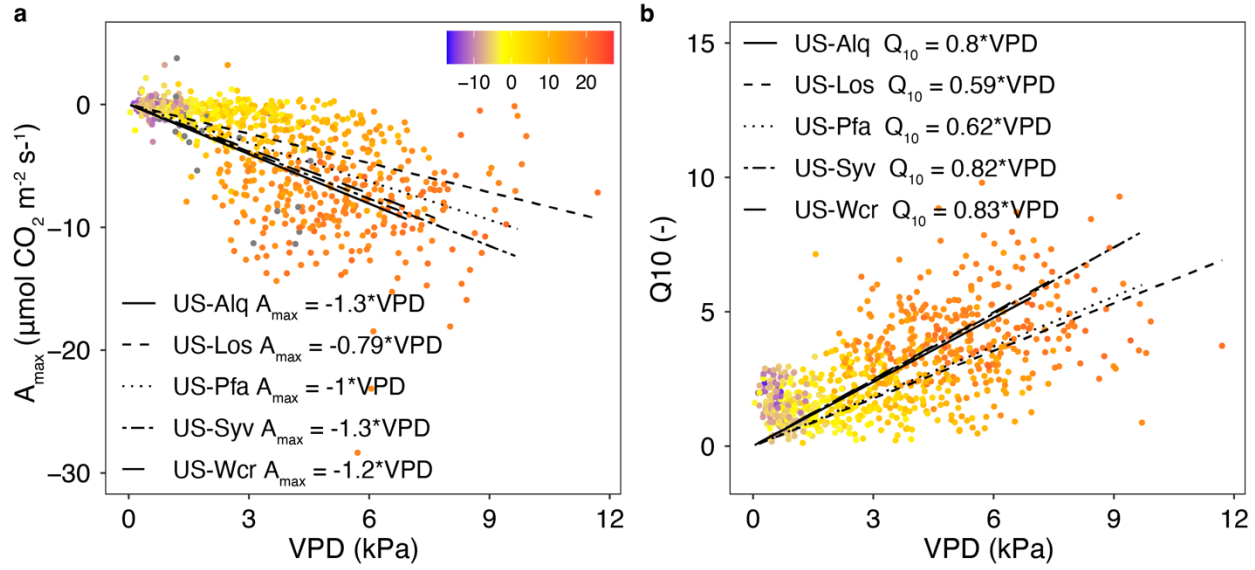


**Figure 9:** Average monthly driver response to NEE fluxes estimated using a mixed model with physiological parameters, with a) differences in growing season (GS) and non-growing season (NGS) NEE by site, b) variations in  $A_{\max}$  by site and its effect on monthly NEE, c) the interaction of site and dark respiration ( $R_d$ ), as well as variations in season and d)  $Q_{10}$ , e)  $A_{\max}$ , and f)  $R_d$  and their effects on NEE.

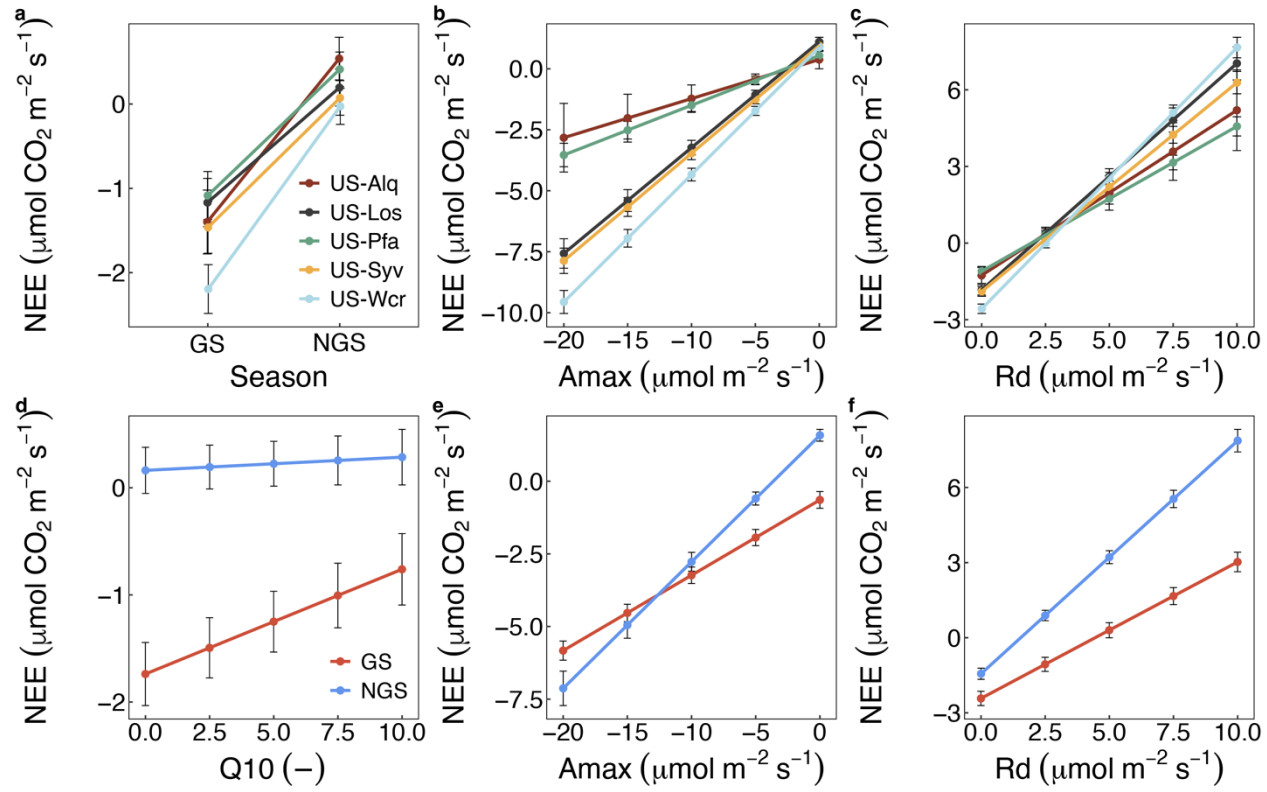


**Figure 10:** Marginal means estimated from the mixed model of monthly  $A_{\text{max}}$  and environmental variables with a) differences between growing season (GS)  $A_{\text{max}}$  and non-growing season  $A_{\text{max}}$  (NGS), b) the interaction of site and vapor pressure deficit VPD (kPa), estimated for data below (dashed) and above (solid) the quantified breakpoint of 7.4 °C, c) the interaction of incoming global radiation ( $R_g$ ) and site, as well as the effect of d) rainfall and e) snowfall below 7.4 °C.

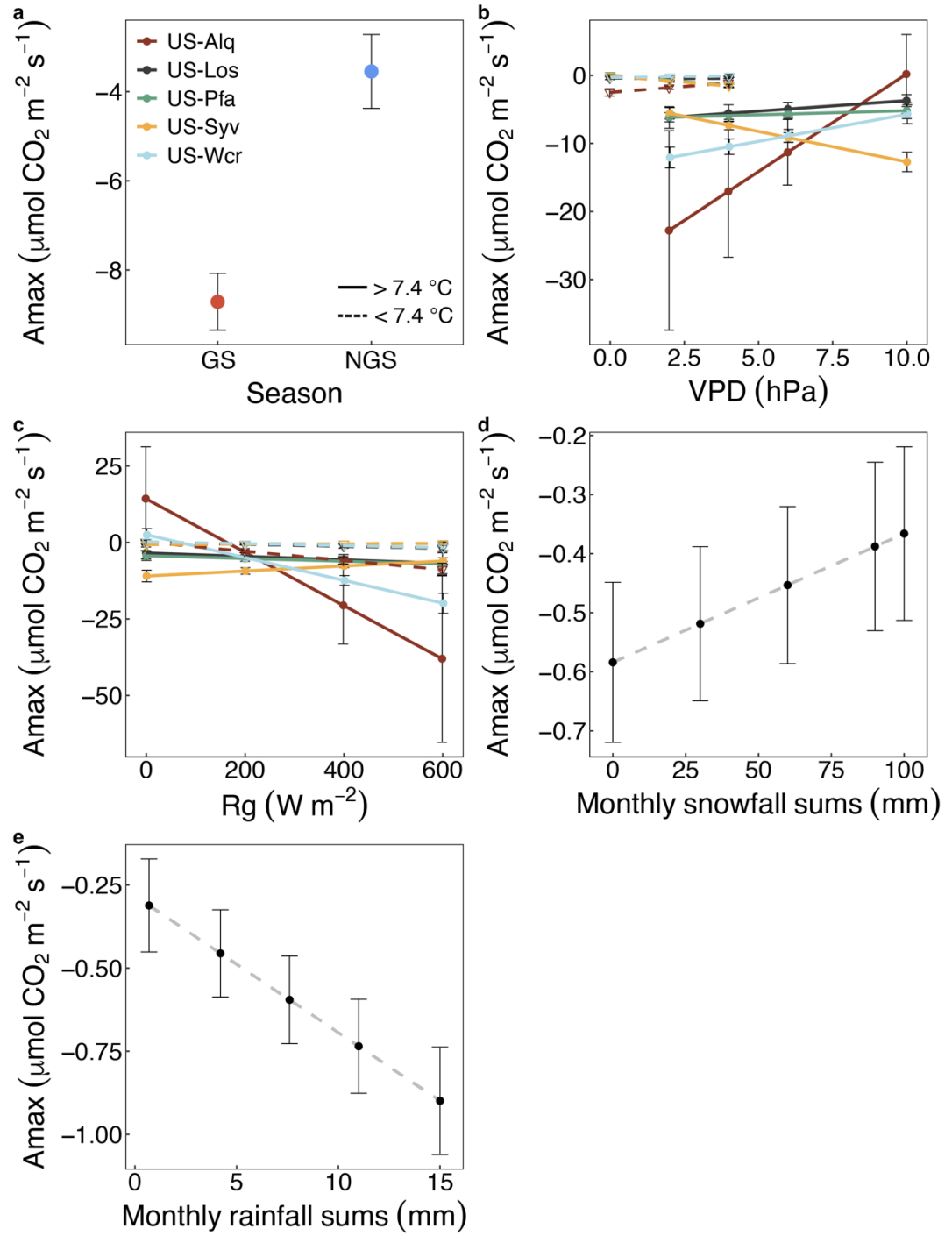


**Figure 11:** Marginal means estimated from the mixed model of monthly aver-

age  $Q_{10}$  and environmental variables with a) differences between growing season (GS)  $Q_{10}$  and non-growing season  $Q_{10}$  ( $N_{GS}$ ), b) growing season vapor pressure deficit in interaction with site, c) the interaction of site and air temperature  $T_{air}$  ( $^{\circ}C$ ), estimated for data below (dashed) and above (solid) the quantified breakpoint of  $-2.2$   $^{\circ}C$ , as well as d) rainfall, also estimated for data below (dashed) and above (solid) the  $T_{air}$  threshold of  $-2.2$   $^{\circ}C$ .

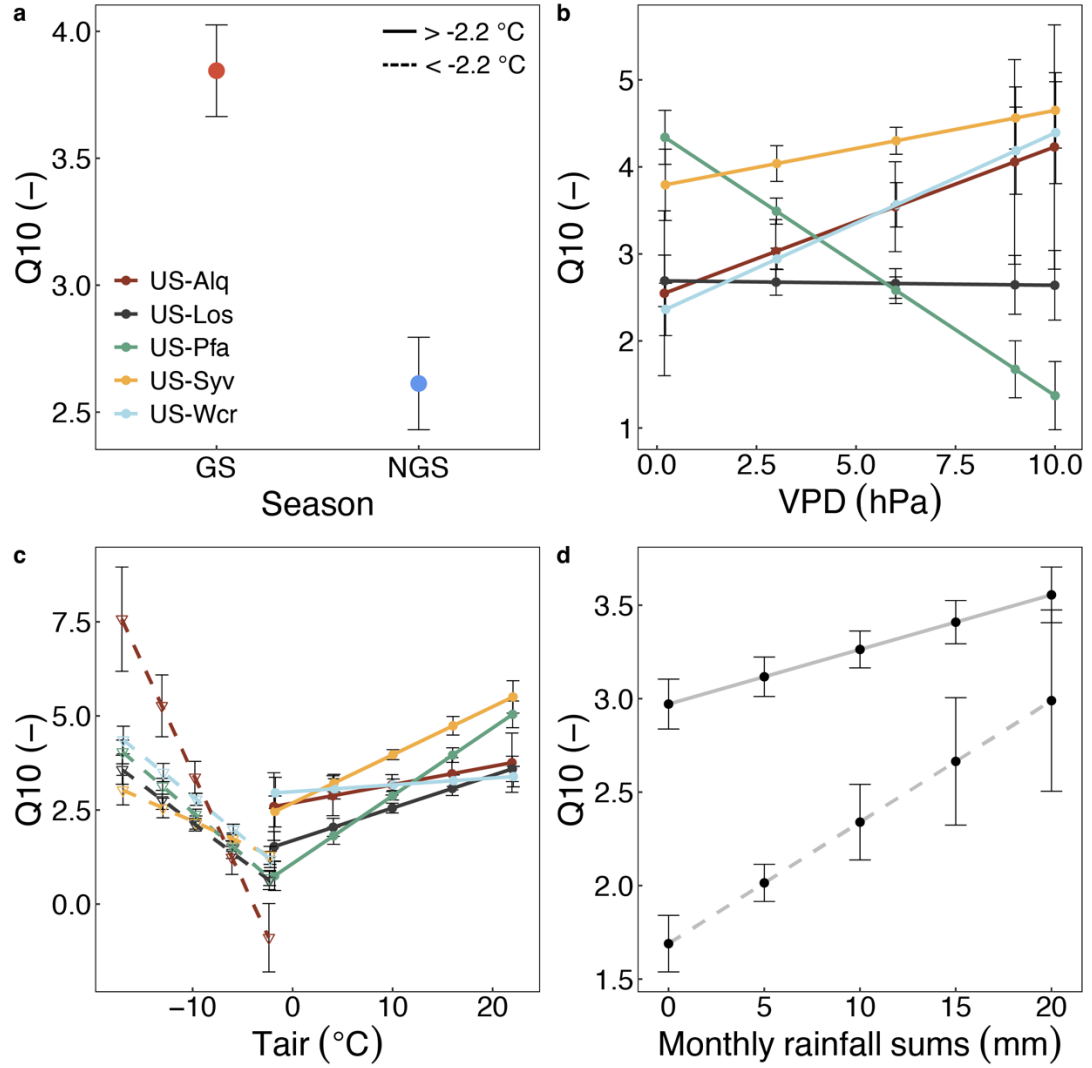


**Figure 12:** Marginal means estimated from the mixed model of monthly average dark respiration ( $R_d$ ) and environmental variables with a) the interaction of site and air temperature  $T_{air}$  ( $^{\circ}C$ ), estimated for data below (dashed) and above (solid) the estimated breakpoint of  $-1.5$   $^{\circ}C$ , as well as b) vapor pressure deficit in interaction with site below  $1.5$   $^{\circ}C$ , and c) the effect of precipitation for data



above 1.5 °C.

